Journal of
Composites Science

MDPI

Review

Valorization of Eggshell as Renewable Materials for Sustainable Biocomposite Adsorbents—An Overview

Bolanle M. Babalola and Lee D. Wilson *

Department of Chemistry, University of Saskatchewan, 110 Science Place, Saskatoon, SK S7N 5C9, Canada; pli912@mail.usask.ca or bolanle.babalola@fuoye.edu.ng
* Correspondence: lee.wilson@usask.ca; Tel.: +1-306-966-2961

Abstract: The production and buildup of eggshell waste represents a challenge and an opportunity. The challenge is that uncontrolled disposal of generated eggshell waste relates to a sustainability concern for the environment. The opportunity relates to utilization of this biomass resource via recycling for waste valorization, cleaner production, and development of a circular economy. This review explores the development of eggshell powder (ESP) from eggshell waste and a coverage of various ESP composite sorbents with an emphasis on their potential utility as adsorbent materials for model pollutants in solid–liquid systems. An overview of literature since 2014 outlines the development of eggshell powder (ESP) and ESP composite adsorbents for solid–liquid adsorption processes. The isolation and treatment of ESP in its pristine or modified forms by various thermal or chemical treatments, along with the preparation of ESP biocomposites is described. An overview of the physico-chemical characterization of ESP and its biocomposites include an assessment of the adsorption properties with various model pollutants (cations, anions, and organic dyes). A coverage of equilibrium and kinetic adsorption isotherm models is provided, along with relevant thermodynamic parameters that govern the adsorption process for ESP-based adsorbents. This review reveals that ESP biocomposite adsorbents represent an emerging class of sustainable materials with tailored properties via modular synthetic strategies. This review will serve to encourage the recycling and utilization of eggshell biomass waste and its valorization as potential adsorbent systems. The impact of such ESP biosorbents cover a diverse range of adsorption-based applications from environmental remediation to slow-release fertilizer carrier systems in agricultural production.

Keywords: eggshell biomass; composite materials; adsorbents; sustainable development; adsorption processes

check for updates

Citation: Babalola, B.M.; Wilson, L.D. Valorization of Eggshell as Renewable Materials for Sustainable Biocomposite Adsorbents—An Overview. *J. Compos. Sci.* **2024**, *8*, 414. https://doi.org/10.3390/jcs8100414

Academic Editors: Ahmed Koubaa, Mohamed Ragoubi and Frédéric Becquart

Received: 14 August 2024
Revised: 9 September 2024
Accepted: 27 September 2024
Published: 8 October 2024

1. Introduction

To address various UN Sustainable Development Goals (UN SDGs 12.5, which targets substantial reduction of waste generation) [1], there is a need to convert generated waste materials into value-added products. Strategies to achieve the UN SDGs include recycling, reusing, or re-channeling waste with concerted efforts to manufacture higher-value products [2]. Over the years, research on eggshell waste has aimed at its greater utilization in a bid to repurpose agriculture waste, such as a soil amendment material to increase the pH and fertility of soil, by high-temperature calcination of eggshells to obtain calcium oxide, CaO [3]. Generally, there are sparse studies on the use of eggshell wastes to cover a range of applications, such as cosmetics [4], cement production [5], polymer and metal composite production [6], as a fertilizer additive, and as a feed supplement for livestock. Furthermore, because of the highly porous nature, estimates indicate that each eggshell contains between 1700 and 7000 pores [7]. In turn, eggshells (ESs) were studied as potential adsorbents for the treatment of contaminated soils and wastewater [8,9].

There is an increasing awareness that the generation of eggshell (ES) waste is rapidly skyrocketing because eggs or its food products are consumed that add to the burgeoning quantity of food waste produced daily, since eggshells are typically landfilled at the consumer levels. From Figure 1, there is a representation of the global egg production, which shows a steady increase in production over several decades and reflects the magnitude of potential amounts of available ES waste. Based on the known wt. content of eggshells, the amount of ES waste in 2019 was estimated as 8.21 M metric tons (equivalent to the weight of 4.1 M passenger cars, based on 10 wt.% for typical chicken eggs). The increasing annual consumption of eggs and disposal of ES waste highlights the need to provide alternative strategies for waste utilization and valorization. Proper management of solid waste is an issue of great environmental concern as the world is currently witnessing high waste generation due to population rise, economic growth, and rapid urbanization. It is estimated that the global urban waste production in 2025 and 2050 will reach 2.2 billion tons and 4.2 billion tons, respectively [10]. Limited availability of resources for environmentally friendly solid waste treatment methods have made solid waste treatment a global challenge [11].

Solid waste treatment technologies can be divided into two broad classes: conventional and non-conventional treatments. The conventional approaches include anaerobic digestion, composting, landfilling, and incineration, while non-conventional approaches include technologies such as pyrolysis, gasification, hydrothermal incineration, liquefaction, etc. [12,13], where such methods reduced the mass (70%) and volume (90%) of the waste to be disposed. Aside from the cost of managing these various technologies and their inherent limitations, the solid waste is generally not targeted for re-use. Valorization of waste is a term used to explain the concept of waste disposal and adding value by converting waste to energy or useful materials. This approach is adopted for preservation of the environment and its natural resources. Valorization of waste may involve biochemical and/thermo-chemical processes. Electricity, heat generation, road construction materials, and soil fertilizers are some examples that highlight the valorization of solid waste.

To improve the sustainability of biogenic ES waste, research on the use of this resource represents a potential opportunity to divert ESs from landfill disposal via recycling and valorization. This includes composite materials that contain ESs, which have potential utility as adsorbent materials for wastewater treatment [14]. Research into the alternative use of ESs as composites was borne from its current supply and availability, along with the projected increase in its consumption, relative abundance, and low cost of ES. Eggshell composites represent a sustainable source of $CaCO_3$ that can serve as a potential biogenic alternative to some non-renewable mineral resources (e.g., limestone) that are currently used as additives for composite materials.

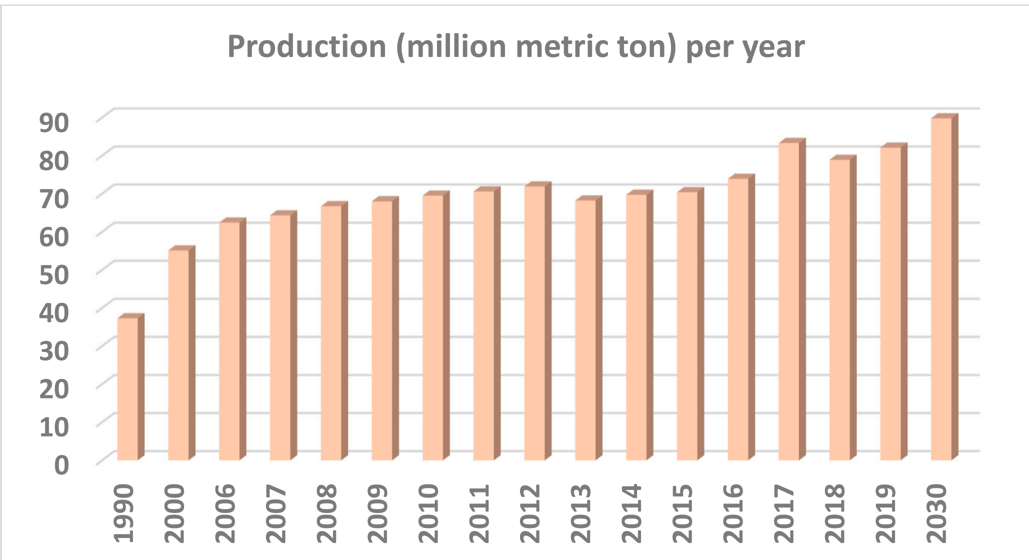

Figure 1. Global egg production for two decades, where production (10^6 metric tons) covers a four-decade period. Redrawn with permission from [15].

Composites offer a modular approach to the utilization of additive materials such as mineral oxides and a means to tailor the physicochemical properties of multicomponent materials [16,17]. ES waste presents a sustainable source mineral oxide that is composed mainly of calcium carbonate (ca. 94 ± 2%), which can serve as a sorbent material (e.g., calcareous soil or calcite) [18,19]. Research has shown that the adsorption mechanism by eggshells occurs mainly by ion exchange, where surface treatment, modification, and functionalization with hydroxyl, amine, amide, or carboxylate groups could improve the adsorbent pollutant capacity. Eggshells in their pristine form or modified by chemical or thermal treatment (by calcination or pyrolysis) have been extensively used to adsorb diverse pollutants such as dyes [20], insecticides [21], metal ions [22], anions [23], and even oxyanions [16,24].

Chicken eggs consist of ca. 10–11% inorganic layer (shell), where the remainder of the weight is the liquid contents. The hard outer inorganic layer of the chicken egg is referred to as the eggshell, which can be brown or white [25]. Calcium carbonate is the main component of eggshells, which also occurs in sedimentary and metamorphic rock formations as limestone or marble [26]. By comparison, eggshells are structurally different from those of marine organisms since the polymorph calcite is formed by poultry. By contrast, the aragonite or vaterite forms that contribute to the formation of sedimentary rocks are also found in marine organisms. There are slight variations in the composition of chicken eggshell depending on the type of feed, but essentially, it is composed mainly of 94 ± 2% calcium carbonate, 1% magnesium carbonate, 1% calcium phosphate, and 3.5 ± 2% organic matter, which is mainly proteins, proteoglycans, and glycoproteins [27–29], and traces of other elements such as Al, K, and S [30]. The ES structure is comprised of three main parts: (i) the cuticle, (ii) the testa or palisade calcite layer, and (iii) the mammillary layer (cf. Figure 2). The cuticle is a thin film, which protects the embryo from moisture loss and infection [31], and is the outermost layer surrounding the eggshell. Next to the cuticle is the testa or palisade calcite layer, which is arranged in columns with small circular pores, where it provides coloration, gaseous exchange, and calcium [26,31]. Thirdly, the innermost layer called the mammillary layer, where there are cones or knobs from organic proteins and are the seeding sites onto which the testa/palisade columns grow [32]. Beneath the mammillary layer are two shell membranes called the outer-shell and inner-shell membranes, where both membranes are assemblies of a network of protein fibers [33].

The study of adsorption isotherms provide insight on the nature of interactions between an adsorbate and an adsorbent material. In the case of dye adsorption, insight on the textural properties and surface chemistry of the adsorbent can be obtained. In terms of equilibrium studies, the maximum adsorption capacity provides a useful metric for comparison of the adsorption efficiency and performance of ES materials with other related adsorbents. Studies of the kinetics of adsorption provide complementary insight on the rate determining steps and mechanistic insight on the adsorption process.

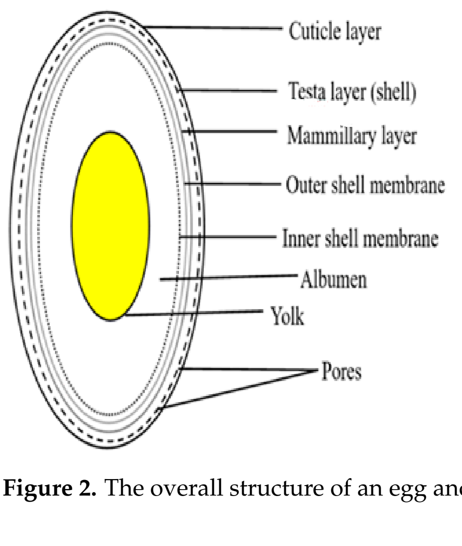

Figure 2. The overall structure of an egg and the eggshell. Copied with permission [26].

This review provides a systematic and a broad coverage of the utility of eggshells as biocomposite adsorbent materials for the removal of pollutants from wastewaters. It explores the utility of eggshell waste and its composites as heterogeneous adsorbents that cover literature over the last decade. This contribution outlines the development of eggshell powder (ESP) and ESP composite adsorbents with an emphasis on solid–liquid systems. Several key topics are described, as follows: (i) isolation of eggshell powder (ESP) in its pristine form and treatment processes; (ii) preparation and materials characterization of ESP biocomposites; and (iii) evaluation of the adsorption properties of ESP and its biocomposites with several classes of model pollutants (cations, anions, and organic dyes) at equilibrium and kinetic conditions. Furthermore, the adsorption isotherms at equilibrium and kinetic conditions for the removal of pollutants reveal the feasibility of adsorption process, in accordance with the thermodynamic and kinetic parameters. This review contributes to the field of biomass utilization via recycling of ESs and valorization of ESP in biocomposite materials for adsorption-based applications. In turn, sustainable development of biocomposite adsorbents contributes to a circular bioeconomy and serve to address various UN SDGs [34]. In particular, the following SDGs are relevant to this research contribution: SDG-6 (water and sanitation), SDG-9 (resilient infrastructure, sustainable industrialization, and innovation), and SDG-12 (waste reduction, recycling, and reuse). The focus on ESP biocomposite adsorbents and their adsorption properties with various categories of pollutants is a key feature of this review. Its novelty lies in the fact that it explores the utility of eggshell waste and its composites with an emphasis on applications as a heterogeneous adsorbent for a wide range of pollutants. This contribution provides coverage of the literature over the last decade.

2. Adsorbent Preparation and Characterization

2.1. Adsorbent Preparation and Modification

The steps are relatively similar among the various studies that describe preparation of the eggshell waste covered in this review. For the preparation of the composites, there are two key unit operations: (i) collection and pre-treatment of ES and (ii) the composite preparation process. A typical preparatory route for eggshells (ESs) obtained from various sources like household waste or industrial wastes require a thorough washing step prior to further processing. Most of the washing (ca. 90%) was performed with purified water or tap water. There are some exceptions since some studies reported the use of chemicals (e.g., ethanol, acetic acid, and sodium hydroxide) for the washing step. One such example was outlined by Lin et al. [35], where the eggshells were immersed in 10% NaOH to remove the shell membranes. Some authors reported the separation of eggshell membranes by mechanical effects during washing, whereas most studies did not report any separation of the membranes. After washing, the ESs were oven dried at variable temperatures (between 100 °C to 120 °C) and duration (between 2 h to 12 h, or longer) prior to grinding. An additional drying step was reported for some of the studies, where the eggshell powder, ESP, was calcined at 500 °C for 3 h to produce calcined eggshell (CES) before eventual utilization in biosorbent preparation. One study reported boiling of the sieved ESP with distilled water for 4 h to remove water-soluble impurities [20]. The dried ES was mechanically crushed into fine a powder (e.g., planetary ball mill, blenders, or mortar), followed by sieving into uniform particle sizes to obtain eggshell powder (ESP), which was stored for further use. A simplified image in Figure 3 illustrates these steps, whereas specific treatments and preparation methods were used to obtain the different eggshell (ES) biocomposite adsorbents shown in the flowchart in Figure 4.

The few steps discussed herein are specific details in addition to the general ES biocomposite preparation steps. The preparation of carbonate hydroxyapatite (CHAP) from ESP was achieved by adding the sieved ESP to industrial H_3PO_4 under controlled conditions, along with filtration. The reaction was completed by adding $Ca(OH)_2$ to the filtered solution, where the resulting dried precipitate is CHAP [36]. The preparation of biogenic $CaCO_3$ (BCa) by inoculating sterilized lysogeny broth liquid medium containing

$CaCl_2$ with *B. subtilis* as a seed liquid was described [37]. The use of oyster shells treated similarly as the crushed eggshells, which was added to NaOH solution and stirred for 2 h, followed by a series of washing and filtration steps until the solution was neutral. HCl was added and stirred for 6 h with filtration to collect the $CaCl_2$ solution, and then mixed rapidly with an equal ratio of sodium carbonate to produce vaterite $CaCO_3$ after drying overnight [38].

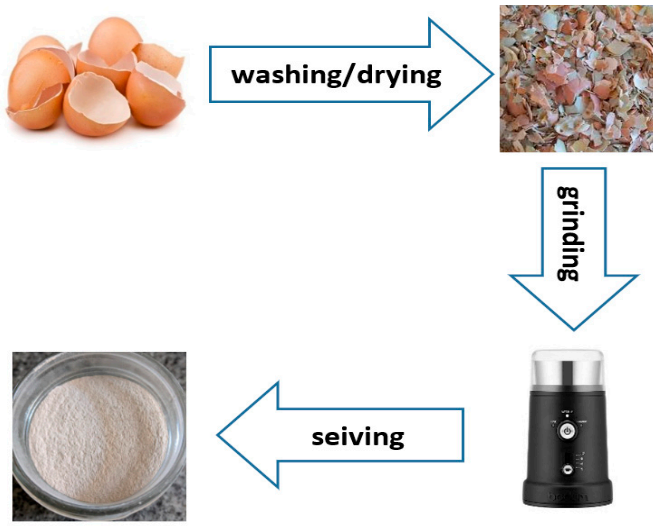

Figure 3. Steps involved in the preparation of ESP.

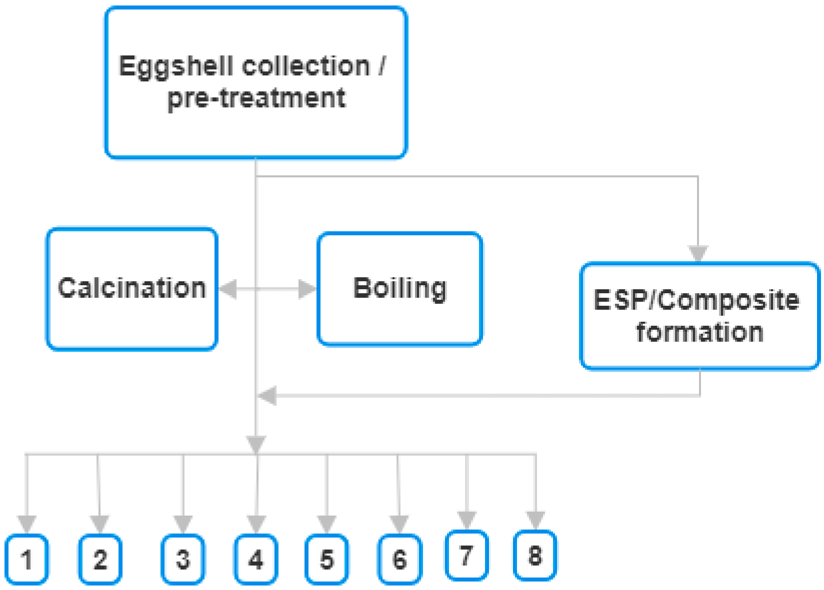

Figure 4. General flowchart of the preparatory steps for making eggshell biocomposite materials that contain various additives (1 to 8), as follows: (1) anthill clay, (2) multi-walled carbon nanotubes (MWCNTs), (3) sodium alginate, (4) titanium dioxide, (5) strontium ferrite, (6) eggshell powder (ESP), (7) sodium dodecyl sulfate (SDS), and (8) chitosan/acetic acid.

Preparation of bentonite/eggshell powder (BEP) adsorbent was achieved by mixing a solution containing ethyl cellulose, polyethylene glycol (PEG) in anhydrous alcohol with ES, and bentonite powders in a 7:3 wt. ratio [39]. Research by Du and Zhu [40] reported that $CaCO_3$ was obtained from starfish by adding commercial protein lyase to a water tank containing starfish kept at 45–50 °C. Then, the bottom precipitate ($CaCO_3$) in the tank was collected, boiled in water, and dried.

The direct surface modification of ESP was respectively carried out with NaOH, HNO_3, and $KMnO_4$ by adding each of the reagents to obtain three different adsorbents denoted as Na-ESP, HN-ESP, and K-ESP [41]. An additional step described herein was required for the preparation of eggshell biochar as a biocomposite adsorbent. Upon mixing ESP with some ground waste plant materials, the mixture was heated up in a furnace [24,37,42,43] to produce BC-1 (biochar from rape straw), BC-2 (biochar rice straw), and BC-3 (biochar from palm fiber). One other method used to produce ES biocomposite adsorbent was achieved by imbibing metal-ions onto the ES surface via physical blending a metal salt (e.g., $AlCl_3$) solution with mixing for 24 h [44].

The literature surveyed did not provide an account or detailed estimation of the cost of producing ESP or composites. Based on previous work of biomass composites, the use of ESP as an additive is anticipated to lower the cost of the input materials of the composite by analogy to agro-waste composites reported by Steiger et al. [16,45]. In the reported studies, the use of biomass additives can amplify the physicochemical properties of biomass composites, which are also inferred in the case of ESP composites.

2.2. Adsorbent Characterization

Eggshell bio composites have been characterized with a range of techniques that are summarized in Table 1 that range from spectroscopy to thermal methods. This includes infra-red (IR) spectroscopy, field emission scanning electron microscopy (FE-SEM) equipped with energy dispersive spectroscopy (EDS), scanning electron microscopy with energy dispersive X-ray absorption spectroscopy (SEM-EDAX), thermal gravimetric/differential thermal gravimetric analysis (TGA/DTA), EDS/SAED (electron diffraction spectroscopy/specific area electron diffraction), TEM/EDS (transmission electron microscopy with EDS), XRD/XRF/EDX (X-ray diffraction, fluorescence, and energy dispersive X-ray), and XPS (X-ray photoelectron spectroscopy). In addition, some studies also report characterization of the ESP biosorbent after the adsorption process. The elemental analysis revealed that ESP has 94% calcium carbonate, 1% magnesium carbonate, 1% calcium phosphate, 3% protein, and 1% organic matter. The average diameter of the ESP particles was 5 µm [46].

Table 1. Characterization of eggshell biocomposite materials.

Type of Characterization/Remarks	Refs
***IR spectroscopy*: About 40% of studies report IR spectroscopy of ESP composite. IR results showed major absorption bands that are strongly associated to the carbonyl and hydroxyl groups. Other IR bands for O-H stretching, C-N-, N-H stretching, and C-H bending were evident in the IR spectra. Sharp bands confirming the presence of CaO, $Ca(OH)_2$, and $CaCO_3$ were observed. The composite revealed characteristic bands depending on the different functional groups present, e.g., Ca-bentonite have signatures for Si-O, Al-O, and O-H. After adsorption, the band appearance became broader and stronger in some composites, while there were minor changes for other materials.	[7,20–24,35,36,41–43,46–58]
***TGA/DTA*: Nearly 20% of the studies considered the thermal stability of the ESP and composite adsorbents. Major decomposition of ES was observed between 460–770 °C, revealing that the upper thermal stability limit of ESP was 630 °C. The minor residual contents of ES show it mainly contains carbonate minerals, whereas complete weight loss occurred between 850 and 920 °C.	[7,21,42,46,50,59–62]
***EDS/SAED*: This method confirms the presence of elements (e.g., K, Ca, Mg, Fe, C, and O) in both ESP and CES. Ca, C, and O have large proportions, revealing that calcium carbonate is the main component of ESP.	[7,46,49,50,53,63,64]

Table 1. *Cont.*

Type of Characterization/Remarks	Refs
***SEM/EDS*:** About 50% of the literature reviewed considered the morphology of the ESP or its composites. In total, 33% of this subset reported the surface morphology after the adsorption process. SEM images reveal that ESP agglomerated and irregular surface features have a porous network and an angular pattern. CES exhibited a macroporous network structure of interwoven cross-linked fibers with diameter between 0.3 and 5 µm. There is increased porosity, and variable surface morphology that depend on the composite components. After adsorption, the structure was crystalline, and pores are no longer visible. EDS showed that Ca, C, and O are major elements in ESP.	[7,20,22,23,36,37,39–41,44,46,48–56,58,60,61,63–67]
***X-ray methods* (*XRD/XRF/EDX*):** X-ray results for ESP is the rhombohedral crystalline phase of calcite showing $CaCO_3$ as the main component that is replaced by CaO after calcination. Patterns also displayed Ca, Si, Na, S, and Mg as the main elements present in ESP. Calcite is the dominant form at or below 800 °C, while portlandite and lime dominate above 800 °C. There is no XRD specific to CaO and $Ca(OH)_2$ in the composites. Variable XRD patterns show the elemental composition of each, for the various CES composites, and additional peaks show the presence of other elemental species. After adsorption, a shift in peak positions were observed in the XRD pattern of ESP depending on the content and composition of the biocomposite and its adsorbed species.	[7,24,37–44,46,50,52,54–56,58–61,63,64,67–70]
***XPS*:** Binding energy values reveal that the main components of ESP and CES as C, Ca, and O. Ca has spectral bands and binding energy similar to $CaCO_3$. Different band are ascribed to Cl 2p and Cl 2s, Pb, PO_4^{3-}, and Ca bands for calcium phosphate appear after adsorption, depending on the adsorbed pollutants.	[24,39,59,69]
***Gas adsorption*:** Surface area pore size analysis (via the BET method):Higher calcination temperature yields a noticeable increase in the surface area, pore volume, and pore diameter of ESP. Combining ESP or CES with biomaterials may improve these properties.	[39,41,42,44,53,54,56,57,59,60,62,67,69]
***Surface charge analysis* (*Zeta potential; mV*):** Ca-bentonite: −12.56 mV; ESP: −17.48 mV; BEP: −16.41 mV; CES: 800 °C = 0.1 mV; 900 °C = 18.1 mV	[39,60]
***Raman Spectroscopy*:** Spectral evidence of graphitic and amorphous or disordered carbon in the composite. The Raman bands of the thin section of ES are characteristic of S-S, amino acids, amide, and C-H groups. After adsorption, new bands specific to the groups of the adsorbate appear.	[53,69]

Prominent signatures from the XRD profile correspond to calcite (using Joint Committee on Powder Diffraction Standards, JCPDS, data), which is the stable form of calcium carbonate at room temperature [46,63]. ESP showed a porous network of agglomerated and irregular surface morphology based on the SEM images, while that of the synthetic sorbents showed greater distribution with high homogeneity of the ultrafine particles with an average size below 50 nm [63]. SEM results showed that the surface consists of nearly round particles, which agglomerate after the adsorption process. TEM and selected area electron diffraction (SAED) analysis revealed a round morphology with length of 98 nm, a width of 34 nm, and non-spotted and non-continuous rings suggestive of non-crystalline powder grains.

SEM characterization of the adsorbent showed that it possessed rough and irregular surfaces with pores of different sizes. The presence of active functional groups and various molecular adsorption sites responsible for adsorption of dye pollutants (MB) were confirmed. Characterization by SEM after the adsorption study revealed that open pores on the initial surface of the composite were blocked after adsorption of the dye molecules [49]. Figure 5 is a combination of spectral results that provide a summary of the materials characterization often obtained for the structural analysis of ESP and its biocomposites.

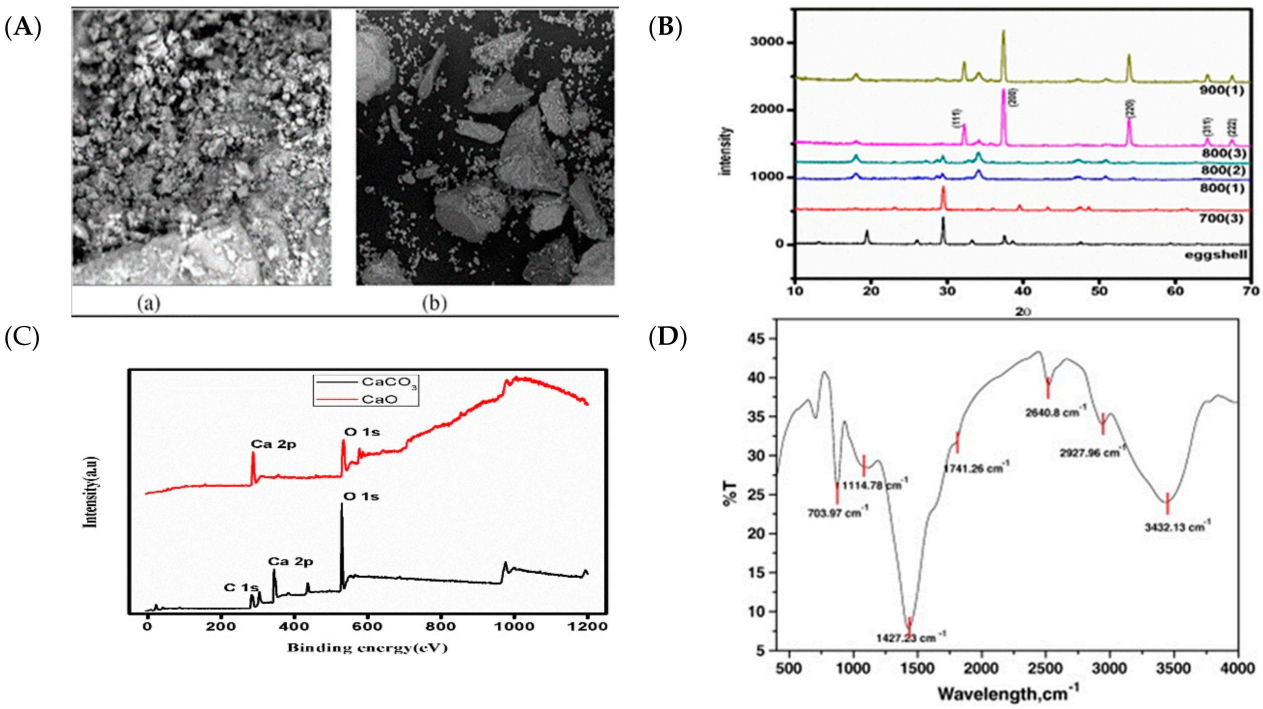

Figure 5. Typical characterization results of ESP. (**A**) SEM: (a) ESP; (b) CES; (**B**) XRD; (**C**) XPS; (**D**) IR copied with permission [7,58,59].

The eggshells were porous with an angular pattern according to the observation from FE-SEM, for copper deposited onto the eggshell, where the SEM image portrayed sheet-like fractured appearance with rod-shaped particles and interlaced pores [65]. For the case of zinc decorated eggshell particles, the image has a greater number of small and interlaced pores. EDS showed that the main component was calcium carbonate, while the metal decorated adsorbents, copper, and zinc were present in addition to the main component of eggshell (calcium, carbon, and oxygen).

The area of coverage of the adsorbent was determined from the plot of the difference between the final and initial optical density of the filtrate after suspending the adsorbent in dye solution at various initial concentration for 45 min and 28 °C at variable adsorbent dosage. In aqueous media, the surface of the ESP-SDS particles has bound water molecules due to hydrogen bonding among the surface sulphate groups with water. One monomer of SDS has an area of coverage of 176 Å^2 with 5–7 molecules of bound water during adsorption, and the tailor-made styryl pyridinium dyes can substitute with the surface bound water. The results reveal that the water molecules around the dye on the ESP-SDS surface decreased with an increasingly hydrophobic chain and a decrease in the area of coverage of the adsorbent [20].

X-ray fluorescence results revealed that the major component of CES is CaO, while traces of other compounds such as MgO, K_2O, Al_2O_3, Fe_3O_4, SiO_2, and SO_2 were also present. Zeta potential (ζ) enables an estimate of the colloidal stability for mixtures, a ζ-value of −25 mV was observed for natural eggshell, whereas a ζ-value of +10 mV was observed for CES, which indicates repulsive and attractive electrostatic attractions, respectively. By comparison, the MWCNTs/CES revealed a slight negative ζ-value with no appreciable adsorption, whereas greater adsorption reveals the involvement of physical forces in the process [71].

TGA results [51] revealed that two weight losses events occurred at two different temperature ranges. The first weight loss of 9.2% relates to removal of calcium hydroxide between 28 °C and 200 °C, and a more prominent weight loss (85.6%) occurred between 200 °C to 570 °C due to decomposition of calcium carbonate to calcium oxide and carbon (IV) oxide [20].

The FTIR results show that the attachment of metals, egg white waste, and dyes did not change the functional groups on the adsorbents, because the density of the immobilized adsorbate was too low for the appearance of specific absorption peak that represents their functional groups [35].

3. Adsorption of Model Compounds by Eggshell Biocomposite Adsorbents

After characterization of the different ESP biocomposites, they were used to treat wastewater containing organic pollutants shown in Table 2, whereas various adsorption studies are highlighted in Table 3 that showcase the utility of these biocomposites as adsorbents. The literature covered on the usage of ESP and its composites as adsorbent materials for pollutant removal in solid–liquid adsorption system were categorized into three distinct groups. The following studies [7,20,21,35,46,48–53,59,62–64,67,69,71] were considered for the adsorption of different dye molecules and other organic pollutants onto ESP and its composites. Adsorption of anions and oxyanions onto ESP adsorbents were summarized [23,24,42–44,54–58,60,61], while for studies including the adsorption of metal ions sorptions [23,36–39,41,61,68,70,72,73].

Table 2. Types of pollutants and their chemical structure.

Common/IUPAC Names	Molecular Structure/Mass/Chemical Formula
Styryl pyridinium dye, 2-(phenylethenyl) pyridinium chloride	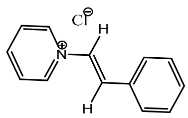 $C_{13}H_{12}N$ 217.69 g/mol
Methylene Blue, MB, Urelene blue, provay blue, 3,7-bis (dimethylamino)-phenothiazin-5-ium chloride	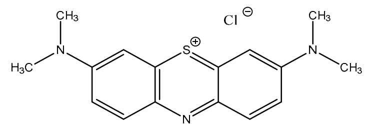 $C_{16}H_{18}ClN_3S$ 319.85 g/mol
Rhodamine Blue, RhB, Basic violet 10, Tetraethylrhodamine 610, 9-(2-carboxyphenyl)-6-(diethylamino) xanthen-3-ylidene-diethyllazanium chloride	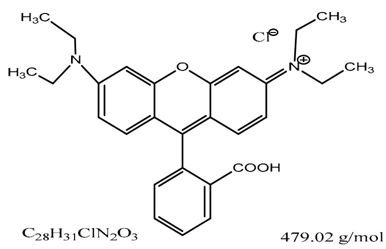 $C_{28}H_{31}ClN_2O_3$ 479.02 g/mol
Toluidine Blue, TB, (7-amino-8-methyl phenothiazine-3-ylidene)-dimethylammonium chloride	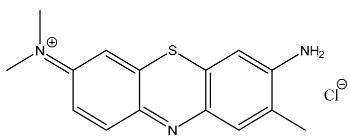 $C_{15}H_{16}N_3SCl$ 270.37 g/mol

Table 2. *Cont.*

Common/IUPAC Names	Molecular Structure/Mass/Chemical Formula
Congo Red, CR, Direct red 28, Benzo congo red, Disodium-4-amino-3-[4-[4-(1-amino-4-sulfonatonaphthalen-2-yl) diazenylphenyl] phenyl] diazinyl-naphthalene-1-sulfonate	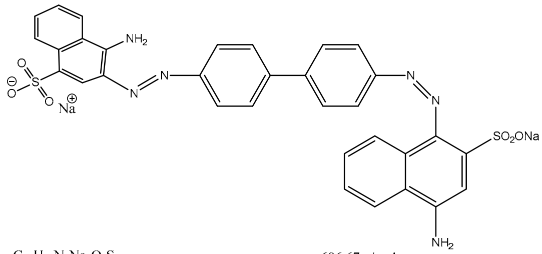 $C_{33}H_{22}N_6Na_2O_6S_2$ 696.67 g/mol
Eriochrome Black T, EBT, Mordant Black 11, Solochrome Black T, Sodium; 3-hydroxyl-4-[(1-hydroxynaphthalen-2-yl) diazenyl]-7-nitronaphthalene-1-sulfonate	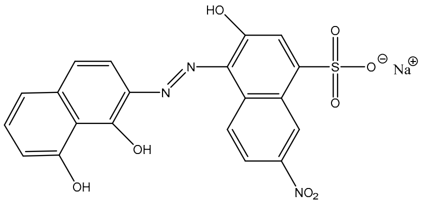 $C_{20}H_{12}N_3O_7SNa$ 461.38 g/mol
Acid Orange, AO7, Orange II, Acid Orange A, Sodium; 4[(2-hydroxynapthalen-1-yl) diazinyl] benzenesulfonate	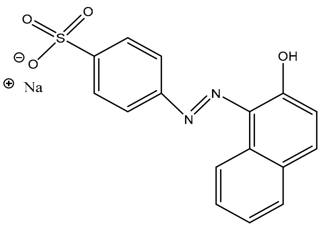 $C_{16}H_{11}N_2NaO_4S$ 350.32 g/mol
Acid red nylon 57, AN57, C. I. Acid Red 57, 6-Amino-5-[[2-[(ethyl phenylamino)sulphonyl] phenyl] azo]-4-hydroxynapthalene-2-sulphonic acid	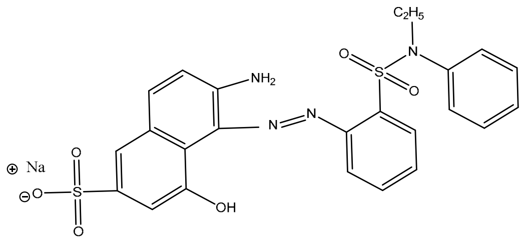 $C_{24}H_{21}N_4NaO_6S_2$ 548.57 g/mol
Methyl red, C.I. Acid Red 2, 2-[(4-(dimethyl amino) phenyl) diazinyl] benzoic acid	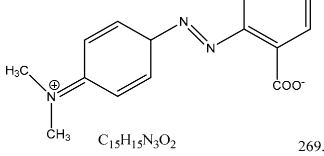 $C_{15}H_{15}N_3O_2$ 269.30 g/mol
Remazol reactive red C.I. 198, Remazol red RB 133, Tetrasodium; 5-[[4-chloro-6-(3-sulfonatoanilino)-1,3,5-triazin-2-yl]amino]-4-hydroxy-3-[[4(2-sulfonatooxyethylsulfonyl) phenyl] diazinyl] naphthalene-2,7-disulfonate	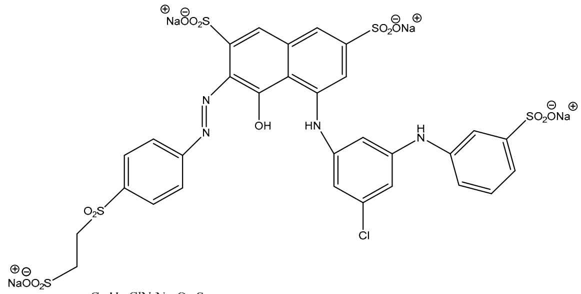 $C_{27}H_{18}ClN_7Na_4O_{16}S_5$ 984.2 g/mol

Table 2. *Cont.*

Common/IUPAC Names	Molecular Structure/Mass/Chemical Formula
Reactive yellow 145 dye, Tetrasodium; 7-[2-(carbamoylamino)-4-[[4-chloro-6-[3-(2-sulfonatooxyethylsulfonyl) anilino]-1,3,5-triazin-2-yl] amino] phenyl] diazinyl] naphthalene-1,3,6-trisulfonate	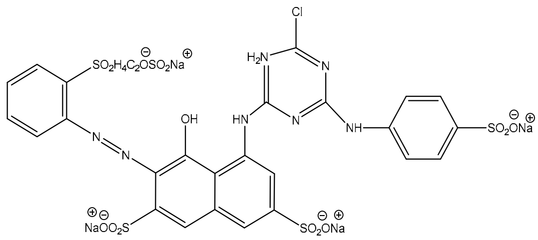 $C_{28}H_{20}ClN_9Na_4O_{16}S_5$ 1026.25 g/mol
Remazol Brilliant Violet 5R dye, RBV-5R, Reactive Violet 5, Trisodium; 5-acetamido-4hydroxy-3-[[2-hydroxy-5-(2-sulfonatooxyethylsulfonyl) phenyl] diazenyl] naphthalene-2,7-disulfonate	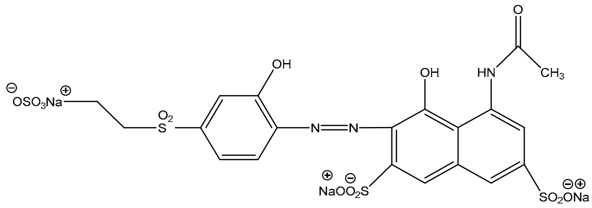 $C_{20}H_{16}N_3Na_3O_{15}S_4$ 735.58 g/mol
Malathion, Carbophos, mercaptothion, 2-[(diamethoxyphosphorothioyl) sulfanyl] butanedioate diethyl	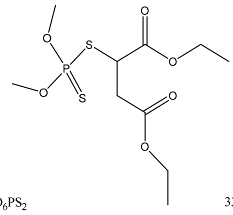 $C_{10}H_{19}O_6PS_2$ 330.39 g/mol
Phenol, Carbolic acid, Phenic acid, hydroxybenzene	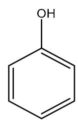 C_6H_5OH 94.11 g/mol
2,4-dichlorophenol (2,4-DCP)	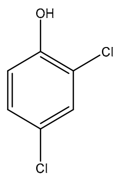 $C_6H_4Cl_2O$ 163 g/mol
Ciprofloxacin, Ciprobay, ciproxan, 1-cyclopropyl-6-fluoro-4-oxo-7-piperazin-1-ylquinolin-3-carboxylic acid	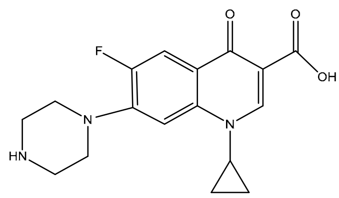 $C_{17}H_{18}FN_3O_3$ 331.35 g/mol

Table 2. *Cont.*

Common/IUPAC Names	Molecular Structure/Mass/Chemical Formula
Tetracycline hydrochloride, Achromycin, Sustamycin, (4S,4aS,5aS,6S,12aR)-4-(dimethylamino)-1,6,10,11,12a-pentahydroxy-6-methyl-3,12-dioxo-4,4a,5,5a-tetrahydrotetracene-2-carboxamide; hydrochloride	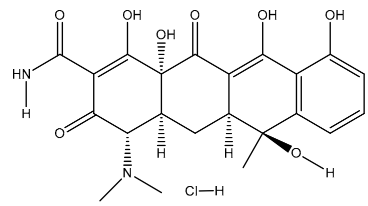 $C_{22}H_{25}ClN_2O_8$ 480.9 g/mol

As shown in Figure 6, a known dosage of ESP biocomposite was applied to treat a known concentration and volume of pollutant, along with mixing for a specified time.

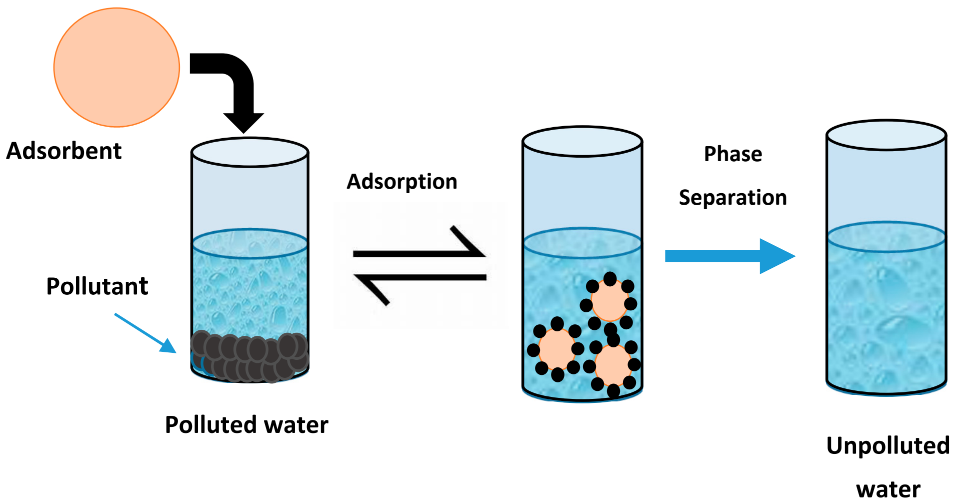

Figure 6. Simplified illustration of an adsorption experiment. Adapted and redrawn with permission [74].

After reaching equilibrium during the adsorption process, the adsorbent was centrifuged or filtered for analysis in order to isolate the residual pollutant solution from the solid phase adsorbent. The experimentally obtained values of the initial adsorbate and residual adsorbate concentration were used to calculate the uptake based on Equations (1) and (2). The uptake results and adsorption parameters from the various studies for the adsorptive removal of cationic and anionic dyes are listed in Table 3.

$$q_e = \frac{(C_o - C_e)V}{w} \tag{1}$$

$$\%\ Adsorption = \frac{C_o - C_e}{C_o} \times 100 \tag{2}$$

where q_e (mg/g) is the amount of pollutant adsorbed per unit mass of adsorbent, C_o and C_e (mg/L) are the initial and equilibrium concentration of the pollutant solutions, V (L) is the volume of the pollutant used, and w is the weight of adsorbent employed.

In all adsorption processes, the equilibrium adsorption capacity, and time-dependent kinetic parameters of the adsorbent–adsorbate system provide insight on the adsorption mechanism. This is necessary for the design, troubleshooting, and optimization of industrial processes [75]. The adsorption isotherms are used to gain insight on the interactions between the adsorbate ions or molecules with the adsorbent active sites, which are expressed by the correlation of the equilibrium data with theoretical or empirical equations [76]. Thus, an isotherm model can be used to describe the relationship between adsorbate and adsorbent at equilibrium. Table 2 shows the structures and names (common/IUPAC) of the organic pollutants removed by ESP. By comparison, Tables 3–5 give a list of models and parameters for consideration when ESP biocomposites are used as adsorbents for organic, cationic, and anionic pollutants.

3.1. Equilibrium Models

For the models described in this section, the context of the adsorption process relates to a solid–liquid heterogeneous process for the case of insoluble adsorbents, where the adsorbate is dissolved in a liquid solvent, which can undergo adsorption at the solid–liquid interface, as depicted in Figure 7.

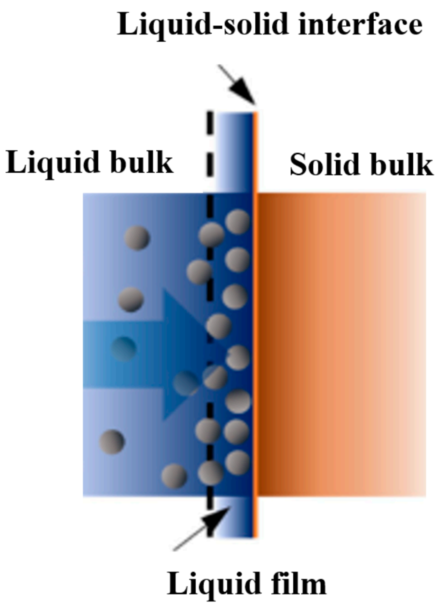

Figure 7. Adsorption of an adsorbate in the liquid phase onto a solid adsorbent at the solid–liquid interface. The circles depict the adsorbate particles while the dashed line represent the imaginary interface boundary. Copied and modified with permission [77].

Isotherm models were tested to determine the *goodness-of-fit* to the experimental results, where different statistical error deviation functions such as correlation coefficient (R^2), the sum of the squares of the errors (SSE), and residual analysis (RESID) are applied to these models [78]. Usually, an isotherm profile showing the relationship between the level of the adsorbed species (adsorbate) onto the adsorbent and the pressure or concentration in case of gas or liquid at constant temperature represents a typical isotherm relationship. The adsorption parameters are estimated by modelling the isotherm data by linearized models as an alternative approach. Some studies compared the linear and non-linear equations, where the non-linear forms are more precise and accurate for parameter estimation [79–82].

Despite the preferred simplicity of linearized models, linearization alters the error functions, error variance, and normality assumptions of the least squares methods [78,83]. Linearization of equilibrium and kinetic expressions is less desirable than non-linear least squares fitting due to bias of error contributions in the slope and intercept parameters for data, especially at low concentration (for equilibrium studies) or short time intervals (for kinetic analysis) [84]. The use of non-linear regression for different models can reduce the statistical bias noted above for linearized models with the same set of adjustable variables [80]. Various isotherm models are known that enable analysis of equilibrium adsorption profiles (e.g., Langmuir, Freundlich, and others), where a wider range of these models have been reported [85–91]. Additional results are presented for the interested readers in the Supporting Material (cf. Section S1). Some examples of important parameters include the adsorption equilibrium constant (K) and the adsorption capacity (q_e). These terms are used to assess the performance of a given adsorbent. These parameters are outlined in Table S1, as outlined below for various classes of adsorbate systems.

The above models represent various isotherm behavior that provide insight on various aspects of the equilibrium process, such as equilibrium adsorption constants, heterogeneity parameters, and energetic terms, which can relate to an enriched view of the adsorption process. By comparison, the time dependence of the adsorption process can be understood by evaluation of kinetic profiles with suitable kinetic models, as outlined in Section 3.2.

3.2. Kinetic Models

Aside from the isotherm models that account for the adsorption profiles at equilibrium conditions, the adsorption profile under non-equilibrium (dynamic) conditions provides insight on the adsorption kinetics and rate parameters of the adsorption process. In simple terms, adsorption kinetics describe the time dependent adsorption of an adsorbate onto the adsorbent versus time. The rate of an adsorption processes is influenced by the contact time, adsorbent surface structure, and initial adsorbate concentration.

Adsorption mass transfer kinetics usually involves some basic steps, which are the transportation of the adsorbate from the bulk of the solution to the adsorbent surface (bulk diffusion), diffusion of the adsorbate into the liquid film (film diffusion), diffusion into the internal pores of the adsorbent (intra-particle diffusion), and the adsorption and desorption of the adsorbates from the adsorbent (surface reaction) [92,93]. An evaluation of the adsorption profile versus time provides insight on the factors that control the rate of the process. Kinetic models can give details about adsorption rates, the performance of the adsorbent, and the probable reaction mechanism to provide a better understanding of the adsorption process, for system design and scale up [94]. The net rate of an adsorption process can be controlled by each step, or a combination of the basic steps involved in the mass transfer, where the rate-determining step may change in the course of the adsorption profile [93].

Some of the methods where contact is achieved between adsorbate and adsorbent in adsorption systems involve batch mode, continuous fixed bed, continuous moving bed, continuous fluidized bed, and pulsed bed. For this review, the batch method and continuous fixed bed method are emphasized. Both methods are low cost, facile, and commonly deployed in research studies. In the batch method, the adsorbate and adsorbent are thoroughly mixed in constant volume of diluted solution while for the continuous fixed bed, the adsorbate is prepared as a solution and allowed to continuously pass through a bed or column packed with adsorbent. The batch adsorption technique requires less volume of dilute adsorbate solution while the fixed bed usually needs more volume and usually of higher concentration of adsorbate. By comparison, the fixed bed method is utilized by industry or other large-scale applications [95] while the batch method analysed by models such as pseudo-first order, pseudo-second order [96] and Elovich models [97] is often applicable for laboratory studies. The fixed bed method is analysed by the Thomas [98,99]; Adams-Bohart [100]; bed depth service time models [101]. Some of the kinetic models used to shed light on the mechanisms involved in the adsorptive uptake of pollutants by ESP are briefly outlined in the Supplementary Materials. The first four kinetic models outlined in Equations [12–17] are mainly used in the batch adsorption process, while other kinetic models shown in Equations [18–24] are applied to fixed bed systems.

Adsorption can occur either via physisorption (weak interactions) or chemisorption (strong interactions). Examples for physisorption are electrostatic interactions (reversible), while chemisorption can occur via coordination through ligand exchange. For specific contaminants, such as phosphate, physisorption via outer sphere coordination or chemisorption via inner sphere coordination (ligand exchange with -OH groups on the adsorbent sites, typically for metal oxides) [102]. The threshold is typically set to 80 kJ/mol for physisorption while chemisorption involves higher enthalpy values above 80 kJ/mol. Section S2 of the Supplementary Materials outline various types of models used in both batch and continuous fixed bed column, along with related parameters that are listed in Table S2.

3.3. Temperature Effects and Thermodynamic Parameters

Temperature effects influence the equilibrium adsorption constant for adsorption processes, along with its role on the rate of adsorption in the kinetics of adsorption. From the isothermal data, it is possible to estimate the thermodynamic parameters, such as standard difference in enthalpy (ΔH°), entropy change (ΔS°), and the change in Gibbs energy (ΔG°) of adsorption for the system of interest. The thermodynamic parameters can be used to determine the driving force of the adsorption process. Thus, the spontaneity or feasibility of a reaction can be ascertained [103,104]. Table 6 provides a summative list of the thermodynamic adsorption parameters typically encountered for ESP and its biocomposites. Positive values of ΔS° values indicate a greater randomness or disorder of the adsorbate at the solid adsorbent–liquid interface. Negative ΔS° indicates decrease level of freedom of the system and reduced driving force for the spontaneous adsorption of the adsorbate onto the adsorbent [105].

In summary, Tables 3–5 provide a list of equilibrium and kinetic adsorption parameters, according to the models described by Equations S1–S22 in the Supporting Material for various adsorbate–adsorbent systems. Table 6 summarizes the thermodynamic parameters of adsorption. The adsorbent materials range from ESP to ES-based composites, whereas the adsorbates range from inorganic to organic species (e.g., metal ions, organic pollutants, oxyanions, anionic pollutants, and dyes). In Table 3, the parameters for model organic pollutants are listed, while Tables 4 and 5 contain parameters for cationic and anionic pollutants, respectively. ES-composites have variable dye adsorption capacity (15.13–303 mg/g) [7,20,35,49,63,64,71], while ES materials (treated or untreated) also display a range values (1.03–600 mg/g) [20,46,48,50–53,59,62]. The metal-ion uptake by ES-composites (5.5–727 mg/g) [72,74] and anion uptake (72.8–231 mg/g), while for ES materials the adsorption values were (0.07–387 mg/g) and (0.1–270 mg/g) for cationic and anionic pollutants, respectively. The adsorption capacity range revealed variable trends in uptake for the ES and ES-based composites depending on the pollutants and type of modification on the composites. Table 7 is a list of some conventional adsorbents used to remove selected pollutants from wastewater and their respective adsorption capacities.

Adsorbent reusability is an important factor to consider in the selection of suitable adsorbent materials for sustainable adsorption-based processes. The ability to regenerate adsorbents affects the overall effectiveness and cost of the process, according to how many cycles of adsorption–desorption can the adsorbent be subjected over its life cycle of application. In view of this, research on the desorption of adsorbed pollutants from ESP and its composites were investigated in previous studies. Desorption of CR from MWCNTs was achieved using 0.5 M HCl [71], while MB and EBT were desorbed from SF/ESP with 5% (*v*/*v*) of NaOH/ethanol, where a desorption efficiency of 45% and 25% were recorded at the fourth cycle [63].

Table 3. Organic adsorbate/ES-based adsorbent systems and their corresponding adsorption and thermodynamic parameters.

Adsorbate	Adsorbent System	Adsorption Parameters	q_e (mg/g) or Removal (%)	Equilibrium and Kinetic Models	Remarks ΔH° = X; ΔS° = Y; and ΔG° = Z	Ref.
Methylene Blue (MB), and Congo Red (CR)	ES matrix (ESP and membrane)	pH 5.23 (MB), pH 7.09 (CR) 1 g/100 mL; 200 rpm; 60 min, 298–343 K	19.8 for MB and 62.1 mg/g for CR	Freundlich and PSO	X = −, Y = − Z = − For CR, Z = negative at 298 and 313 K.	[48]
RhB, Murexide, and Eriochrome black T (EBT)	CES	pH 5; 0.25 g/50 mL; 90 min; 2 mg/L dye solution	(RhB) = 2.0, (Murexide) = 1.03 and (EBT) = 1.56	Langmuir, Dubinin-Radushke-vich (D-R), and PSO	EBT has the highest reported adsorption	[46]

Table 3. *Cont.*

Adsorbate	Adsorbent System	Adsorption Parameters	q_e (mg/g) or Removal (%)	Equilibrium and Kinetic Models	Remarks ΔH° = X; ΔS° = Y; and ΔG° = Z	Ref.
Cu^{2+}, Zn^{2+}, Ni^{2+}, Co^{2+}, and soluble microbial product (bovine serum albumin, BSA)	ESP ESP-metal composite, ESP-M, was adsorbent for BSA	5 g, 25 mL, 20 rpm, 25 °C, 24 h 0.2 g, 5 mL BSA in sodium acetate buffer.	q_e (BSA) by ESP-M are listed: ESP-Zn = 32.6 ESP-Cu = 30.1 ESP-Co = 2.6 ESP-Ni = 0.3	Sips and PSO	Zn showed higher binding to ESP than other metal ions. At investigated temperatures [277–323 K), ΔH° = +, ΔG° = −, ΔS° = + Good desorption of BSA was achieved with EDTA	[67]
Acid Orange 7 (AO7) Toluidine Blue (TB)	ESP decorated with Zn metal waste and chicken egg white (ESP/Zn/CEW) Eggshell decorated with Cu metal waste and chicken egg white (EPS/Cu/CEW)	pH 2 (AO7) pH 12 (TB); 5.0 mg/mL dye solution; 0.2 g/5 mL; 100 rpm; (AO7) took 30 min on ESP/Zn/CEW and 120 min on ESP/Cu/CEW, TB was 5 min for both adsorbents	(AO7) by ES/Zn/CEW = 64.10, (AO7) by ES/Cu/CEW = 100.56, (TB) by ES/Zn/CEW is 115.15 and (AO7) by ESP/Cu/CEW = 100.56	Sips and PSO	Unsatisfactory result with the elution of AO7 from ES/Zn/CEW but 71.3% was recovered with ES/Cu/CEW. For TB, nearly 100% recovery from both adsorbents by using 50% glycerol mixed with 1 M $(NH_4)_2SO_4$ as eluent.	[35]
Eriochrome black T (EBT), Methylene Blue (MB)	ESP; Strontium nanoferrites (SF), SF/ESP composite	EBT@ pH 2 MB @ pH 8; 0.05 g/50 mL; 100 mg/L; 150 rpm ESP is 90 min SF is 65 min SF/ESP is 40 min 298–328 K	(EBT) by SF = 39.12; (EBT) by SF/ESP = 42.52; (MB) by SF = 37.61; (MB) by SF/ESP = 42.26	Langmuir and PSO	ΔH° = +, ΔS° = +, ΔG° = −. EBT desorption was achieved with 5% (*v*/*v*) 0.1 M NaOH/ethanol. Good MB desorption was obtained with 5% 0.1 M acetic acid/ethanol. Adsorbent re-usability declined (<40%) at the 4th cycle.	[63]
Tailor-made styryl Pyridium dye (addition of alkyl chains and different sub-stituents)	Eggshell modified with sodium dodecyl sulphate (ESP-SDS)	200 mg; 294–318 K	15.13–303.00	Freundlich and PSO	q_e depends on the type of dye substituents and chain length. Higher q_e were obtained for dyes with longer hydrophobic ends and stronger electrophiles (-Cl, -OMe, $-NMe_2$). ΔH°, ΔS°, and ΔG° = negative	[20]
Methylene Blue (MB)	Eggshell and anthill clay (ESPAC)	0.2 g/100 mL; 150 rpm, 30 °C	23.87	Freundlich and PSO	Central Composite Design CCD of the response surface methodology was involved in the experiment. There was correlation between the actual and the predicted responses.	[49] **
Congo Red (CR)	ESP, CES, MWCNTs/CES	50 min for ESP 40 min for CES and MWC-NTs/CES; 0.5 g/25 mL for ES, 0.05 mg/25 mL for CES and 0.02 g/25 mL for MWCNTS/CES; 100 mg/L dye solution; 293–333 K.	5.76 for ESP; 58.14 for CES; 136.99 for MWCNTs/CES	Langmuir and PSO	Result from pH were not stated. Good desorption was achieved with 0.5 M HCl. ΔH° = −, ΔS° = − ΔG° = −.	[71]

Table 3. *Cont.*

Adsorbate	Adsorbent System	Adsorption Parameters	q_e (mg/g) or Removal (%)	Equilibrium and Kinetic Models	Remarks ΔH° = X; ΔS° = Y; and ΔG° = Z	Ref.
Acid dye red nylon 57 (AN57)	Calcined eggshell decorated with sol gel TiO_2 (TiO_2/CES)	pH 3; 40 min; 100 mg/L; 200 rpm; 0.05 g/10 mL; 298–328 K.	220.2	Langmuir and PSO	Excellent desorption with 0.5 M HNO_3. ΔH° = −, ΔS° = −. ΔG° = −.	[64]
Methyl red dye (MR)	ESP	pH 2; 180 min; 8 g/300 mL; 25 °C; 20 mg/L dye solution; 298–328 K	1.66	Langmuir and PSO	ΔH° = +, ΔS° = +, ΔG° = −	[51]
Remazol red 198 dye	Eggshell immobilized with polymer matrix of alginate and poly vinyl alcohol	pH 1; 180 min, 10 g/L; 500 rpm; 295–323 K	46.9	Freundlich and PSO	ΔH° = −, ΔS° = −, ΔG° = −	[7] **
RBV-5R	ESP	pH 6; 700 rpm; 293 K; 20 mg/L dye level; 1.5 g/100 mL solution	9.94	Langmuir and PSO	Photocatalytic degradation with P25 (TiO_2) catalyst	[53]
Reactive yellow 145 (RY 145), Cadmium	ESP	pH 2, RY145, pH 5, Cu; 150 mg/L; 80 min; 150 rpm; 303–318 K	88.45 for RY145 101.5 for Cu	Freundlich, Sips, Redlich-Peterson, D-R, and PSO	ΔH° = +, ΔS° = −, ΔG° = −	[50]
Malathion	CES	0.6 g, 100 mL, 300 ppm, pH 6, 2 h	318.5	Langmuir and PSO	Above 90% desorption was achieved at 500 °C until after the third cycle	[21]
MB, TB	CES	pH 7, 20 ppm, 50 mg, 50 mL, 15 min for MB and 10 min for TB	17.35 MB, 16.22 TB	PSO	83% degradation efficiency obtained at the 5th cycle with acetone. Photodegradation was employed; Chitosan-ESP showed reduced degradation efficiency	[59]
Phenol	ESP	3.5 g, pH 9, 25 °C, 15 mg/L	0.45	Freundlich and PSO	ΔH° = −, ΔS° = +, ΔG = −	[52]
2,4-dichlorophenol (2,4-DCP); (RhB); ciprofloxacin (CIP); tetracycline. HCl (TCH); Phenol (Ph)	CES	5 mg, 30 mL, 100 mg/L, 120 min, 30 mg/L persulphate (to activate reaction)	540, 600, 420, 510 and 570 was obtained for 2,4-DCP, RhB, CIP, TCH and Ph, respectively	PSO	70% removal with ethanol and could increase to 80% after recalcination at 500 °C for 2 h	[69]
Phenol	CES without membrane (CES1); CES; calcined membrane (CEMemb)	500 mg, 50 mL, pH 5.7, 150 rpm, 25 °C, and 48 h	CES1 =119; CES = 143; CEMemb = 192	Langmuir, Sips, and Redlich-Peterson	ΔH° = −, ΔS° = −, ΔG° = −	[62]

** indicates a non-linear model was used.

Table 4. Equilibrium and kinetic adsorption parameters of ESP/composite for heavy metal ions in wastewater systems.

Pollutants	Adsorbents	Adsorption Parameters	q_e (mg/g)	Equilibriumand Kinetic Models	Remarks	Ref.
Pb^{2+}, Cu^{2+}	ESP, banana peel powder (BPP) Pumpkin powder (PP)	pH 7, 0.1 g, 90 min, 100 mL, 5 ppm, 100 rpm	Not reported (NR)	NR	Pb^{2+} had higher adsorption than Cu^{2+}	[72]
Al^{3+}, Fe^{2+}, and Zn^{2+}	ESP, membrane biological reactor (MBR)	10 g, 1 L containing 12 ppm Zn^{2+}, 6 ppm Al^{3+} and 6.5 ppm Fe^{2+}, 2 h, 500 rpm 25 °C	60 Al^{3+} 48.1 Fe^{2+} 70.8 Zn^{2+}	NR	ESP, and in combination with MBR. ESP was more selective to Al^{3+}	[106]
Pb^{2+}, Cu^{2+}, Zn^{2+}, Cd^{2+}	Chitosan (Ch), sugar beet factory lime (SBFL), ESP, humate potassium (HK)	2 g, 40 mL, 24 h, room temp	0.01 Cd^{2+}, 8.1 Cu^{2+}, 2.2 Zn^{2+}, Pb^{2+} was not detected	Freundlich and PSO	Ch > SBFL > ESP > HK. Cd^{2+} removal was higher in HK and Ch	[107]
Fe^{3+}, Cu^{2+}, Zn^{2+}, Mn^{2+}, AsO_3^-, Cd^{2+} (from AMD)	Calcined eggshells (CES), microalgae, *Chlorella vulgaris*	3.0 g/L, 30 min, and 40 L	6.25 Cu^{2+}, 5.29 Zn^{2+}, 2.78 Mn^{2+}, 0.1 AsO_3^-, 0.07 Cd^{2+}, 36.78 Fe^{3+}	NR	The hybrid system removed 99–100% of all the metal ions	[66]
Fe^{3+}, Pb^{2+}, Zn^{2+}, Cu^{2+}, Ni^{2+}, Cr^{6+} from landfill leachate	CES in column experiment preceded by a coagulation-flocculation (CF) process	2.0 mL/min, 11 min EBCT, pH 6.8, 25 °C, 11 days operational time and 25.5 g.	3.93 Fe^{3+}, 0.45 Pb^{2+}, 4.6 Zn^{2+}, 1.24 Cu^{2+}, 1.33 Ni^{2+}, 0.89 Cr^{6+}	Thomas, Yoo-Nelson, Adams-Bohart	CES column is comparable with granular activated carbon (GAC)	[108]
Cu^{2+}, Cd^{2+}, Pb^{2+}, Cr^{6+}, Zn^{2+}	$CaCO_3$ from starfish, conventional adsorbents: commercial $CaCO_3$, crab shell, sawdust, activated carbon	5 g, 1 L, pH 7, 3 mg/kg, 20 °C, 20 min column residence time	0.52 Cu^{2+}, 0.57 Cd^{2+}, 0.49 Cr^{6+}, 0.52 Zn^{2+}, 0.47 Pb^{2+}	PSO	Adsorbents showed excellent removal (%). $CaCO_3$ from starfish was the highest. Desorption was higher using 5 or 7 M HNO_3 versus NaOH	[109]
Pb^{2+}, Cd^{2+}, Zn^{2+}	Mollusk shell powder in aragonite phase (razor clam shells, RSC), and calcite phase (oyster shell powder, OS)	20 mg, 150 mL, pH 6, 48 h, 25 °C	RSC: 553.3 Zn^{2+}, 656.8 Pb^{2+}, 501.3 Cd^{2+}; OS: 564.4 Zn^{2+}, 1591.3 Pb^{2+}, 120.3 Cd^{2+}	Freundlich	Both BCa sorbents showed similar sorption capacities for Zn; OS had higher sorption for Pb, while both had low sorption for Cd	[40]
Cd^{2+}, Pb^{2+}, Cu^{2+} from AMD	ESP	pH 2.4, Effluent flow rate = 10 mL/min, bed depth = 10 cm; 0.39 mg Cd^{2+}/L; 1.2 mg Pb^{2+}/L; 6.3 mg Cu^{2+}/L	1.57 Cd^{2+}, 146.44 Pb^{2+}, 387.51 Cu^{2+}	Thomas, BDST, Adams-Bohart	% desorption with 0.1 M HNO_3: 52.1–86.9% Cd^{2+} 18.3–46.5% Pb^{2+}, 34.3–58.9% Cu^{2+}	[68]

Table 4. *Cont.*

Pollutants	Adsorbents	Adsorption Parameters	q_e (mg/g)	Equilibriumand Kinetic Models	Remarks	Ref.
Solution of Ni^{2+}, Cu^{2+}, Cd^{2+}	Clay limestone, WM, ESP, eggshell after hatching, ESH	1 g, 200 mL, 3 h, 500 rpm, pH range 4.6–5.4	NR	PSO		[110]
Pb^{2+}	Surface modified eggshell powder with: NaOH, Na-ESP; HNO_3, HN-ESP; $KMnO_4$, K-ESP	50 mL, pH 5, 150 mg/L, 10 mg, 1 h, room temp.	K-ESP had 727.5; Na-ESP had 375, HN-ESP had 150	Langmuir and PSO	The confidence level using central composite design, CCD, is above 95%. $\Delta H^\circ = +$, $\Delta S^\circ = +$ $\Delta G^\circ = -$	[41]
Pb^{2+}, Cr^{3+}, Fe^{3+}, Cu^{2+}	Vaterite $CaCO_3$ from oyster shells; Commercially available $CaCO_3$	30 mg, 30 mL, 1000 ppm, 60 min	999 Pb^{2+}, 995 Cr^{3+}, 993 Fe^{3+}, 571 Cu^{2+}.	NR	Pb^{2+} was tested with commercial $CaCO_3$ and 78% was adsorbed, Lead removal (%) in real wastewater was 95.1%	[65]
Pb^{2+}, Cu^{2+}, Zn^{2+}, Cd^{2+}	Bentonite and ESP, BEP, Ca-bentonite	1.0 g, 50 mL, 200 mg/L, 3 h, 25 °C	9.99 Pb^{2+} and Cu^{2+}, 6.0 Cd^{2+} and 5.5 Zn^{2+}	Elovich	In a mixed metal solution, the removal order was $Cu^{2+} > Pb^{2+} > Zn^{2+} > Cd^{2+}$. The composite has 96.90%	[39]
Pb^{2+}	Carbonate hydroxyapatite (CHAP) from ESP	pH 6.0, 60 min, 101 mg/g, 225 rpm, 200 mg/L	94.5 mg Pb (II)/g CHAP	NR		[36]
Pb^{2+}	Mechanochemical activation of $CaCO_3$	$CaCO_3$/Pb (II) at 1:1, M^{2+}/Pb (II) at 1:1, 90 min, 300 rpm	Above 99% removal was recorded	NR	The efficiency of removal for Zn^{2+}, Mn^{2+}, Ni^{2+}, Cd^{2+}, was less than 1%	[111]
Cd^{2+}	ESP	150 mg/L, 75 min, 0.75 g, pH 6, room temp.	146 mg/g	Freundlich and PSO	Central composite design (CCD) was employed for optimization	[22]
Cd^{2+}	$CaCO_3$ induced by *Bacillus subtilis*, BCa, abiotic $CaCO_3$: limestone and Analytical reagent grade AR-$CaCO_3$	pH 5, 25 °C, 196 mg/L	BCa had 172.41; AR-$CaCO_3$ had 6.31; limestone had 21.01; *Bacillus subtilis* debris had 40.82	Langmuir and PSO		[37]
Cr^{3+} from real chrome tanning waste-water	ESP, marble powder	pH 3.81, 20 g/L ESP, 12 g/L marble powder, 3.21g/L, 14 h for ESP, 30 min for powdered marble, 250 rpm, and 50 mL	159 ESP, 262 powdered marble	Langmuir and PSO	$\Delta H^\circ = +$, $\Delta S^\circ = +$ $\Delta G^\circ = -$	[112]

Table 4. *Cont.*

Pollutants	Adsorbents	Adsorption Parameters	q_e (mg/g)	Equilibriumand Kinetic Models	Remarks	Ref.
Cu^{2+}	Co-grinding copper sulfate solution with $CaCO_3$	pH 5.61, Cu (II) was 0.001 mol/L, $CaCO_3/Cu^{2+}$ at 1:1, 100 min milling, 300 rpm, 10% milling balls	The removal is 99.76%		Ni^{2+}, Mn^{2+}, Zn^{2+}, Cd^{2+} present remained in solution at about 94.7%, 98.8, 75.2, and 84.5%, respectively	[70]
Cu^{2+} from sulfate bearing wastewater	Co-grinding wastewater with $CaCO_3$; with solutions of $Cu(NO_3)_2$, $CuCl_2$	300 mL, 300 mg/L, 200 g milling beads, 30 min, Ca/Cu^{2+} was 1:1	99% Cu^{2+} removal with $CaCO_3/Cu^{2+}$; 13% with NO_3^-, 33% with Cl^-			[73]
Cu^{2+}, Mn^{2+}, Zn^{2+}, Ni^{2+}	Mechanically activated $CaCO_3$	1 mM MSO_4 solution, Ca/M^{2+} molar ratio is 1:1, 230 rpm, 100 min, 200 g milling balls	Recovery of Cu^{2+} and Zn^{2+} were 99 and 53% respectively while Ni^{2+} and Mn^{2+} were below 5%	PSO		[38]

The bulk of the literature examined in this review focused solely on single component adsorbate systems. In environmental and industrial wastewater, the role of multicomponent species can affect the adsorption efficiency of other ions due to competitive adsorption. For example, the presence of chloride ions in the solution, especially at higher concentration, negatively affected the removal of nitrate ions due to the competitive effects for similar active sites on the adsorbent surface [42]. Hu et al. [113] reported that chloride ions are able to adsorb quickly onto the available sorption sites, thereby increasing the electrostatic repulsion forces between nitrate and the sorbent. Competitive ions in solution drastically reduced the distribution coefficient (K_d) of the metal ions when compared to single component metal ion systems. K_d is a representation of their mobility or partitioning and distribution properties between the solid and liquid phase, where a higher K_d indicates a greater distribution into the solid phase and vice versa [107].

Table 5. Adsorption of ESP/composite for anions in wastewater systems.

Adsorbate	Adsorbent System	Adsorption Parameters	q_e (mg/g)	Equilibrium and Kinetic Models	Remarks	Ref.
PO_4^{3-}	CES	5 g, 2 mg/L, 100 mL, 25 °C, 100 rpm, 2 h	3.68	Langmuir	80% removal with real wastewater	[56]
$H_2PO_4^-$	ESP, CES	25 mL, 100 mg/L, pH 5, 0.05 g, 24 h	ESP =178.6; CES = 270.3	Langmuir	Co-anion reduced the adsorption capacity of both biosorbents thus: $Cl^- \sim NO_3^- < SO_4^{2-} << HCO_3^-$	[57]
CN^-	CES	pH 7, 10 mL, 0.01 M	3.27 mg/g	Langmuir		[58]

Table 5. *Cont.*

Adsorbate	Adsorbent System	Adsorption Parameters	q_e (mg/g)	Equilibrium and Kinetic Models	Remarks	Ref.
PO_4^{3-} and SO_4^{2-} in slaughter wastewater (SWW)	Syn. $Ca(Ac)_2$ from ES	pH 12, 465.75 mg SO_4^{2-}/L, 856 mg PO_4^{3-}/L, 50 mL, 0.175 g	86.2 mg SO_4^{2-}/g, 99.1 mg PO_4^{3-}/g.	PSO	High removal of TSS, metal ions, fecal, and coliforms.	[55]
F^-	CES	pH 7, 25 °C	258.28	Langmuir and PSO	Co-anions decreased adsorption in this order: HPO_4^{3-} > HCO_3^- >> SO_4^{2-} > Cl^- ΔH° = +, ΔS° = +, and ΔG° = −.	[60]
F^-	ESP	100 mL, 250 rpm, 1 h, 0.5 g, 303 K, and pH 6	1.09	Langmuir and PSO	ΔH° = −, ΔS° = −, and ΔG° = −	[23]
NO_3^-	ESP, BC-3, nZVI-BC-3, CES-BC-3	40 mL, 200 mg/L, 150 rpm, pH 5, 24 h, and 1 g/L	nZVI-BC-3 has 148.1, CES-BC-3 has 72.77	Freundlich and PSO	Decreased sorption due to co-existing chloride: nZVI-BC-3 < ESP-BC-3 < CES < BC-3	[42]
PO_4^{3-}	ESP, ESP-Al	100 mL, 0.1 g ESP-Al in 5 mg (P)/L, 10 mg (P)/L in 1 g ESP, 200 rpm, and 313 K	ESP, ESP-Al respectively has 0.57 and 6.23 mg(P)/g	Langmuir and PSO		[44]
PO_4^{3-}	RS, BC-1, CES-BC-1	0.05 g, 50 mL, 200 mg P/L, 180 rpm, 25 °C, and 24 h	RS = 2.173, BC-1 = 101.0, CES-BC-1 = 109.7	PSO		[43]
HPO_4^{2-}	CES	30 mL, 0.3 g, 600 mg P-PO_4/L, pH 8, 25 °C, 2 h, 100 rpm		Sips and PSO		[61]
HPO_4^{2-}	RS, BC-2 CES-BC-2	0.01 g. 40 mL, 220 rpm, pH 7, 298 K	CES-BC-2 has 231	Langmuir and PSO	Co-existing anions affect the trend in uptake: HCO_3^- > SO_4^{2-} > NO_3^- > Cl^- ΔH° = +, ΔS° = +, and ΔG° = −	[54]
PO_4^{3-}	CES, PES, PES-BC-3	20 mg, 200 rpm, 2 h, 200 mg P/L	PES-BC-3 has 109.7	Langmuir and PSO	CES < PES < PES-BC-3	[24]

Table 6. Thermodynamic parameters for the adsorption of pollutants onto ESP/composite in wastewater systems.

Adsorbate-Adsorbent Systems	Temp. (K)	ΔH° (kJ/mol)	ΔS° (J/mol.K)	ΔG° (kJ/mol)	Ref
Remazol red 198-immESP	295	−3.33	−7.95	−973.9	[7]
Styryl pyridinium dye -ESP-SDS	300	69.3	281.3	15.3	[20]
F^-ESP	303	−58.15	−0.16	−9.01	[23]
CR-ES matrix	298	−22.61	−70.86	−1630.1	[48]
MB-ES matrix	298	−63.04	−185.79	−8949.3	[48]
Pb^{2+}-ESP	295	55	209.3	−6.58	[41]
Cd^{2+}-ESP	303	26.28	86.57	−49.2	[50]
RY4-ESP	303	18.02	60.16	−251.8	[50]
MR-ESP	298	31.90	150	−11.6	[51]
Phenol-ESP	295	−388.9	1.65	−7.40	[52]
HPO_4^{2-}-CES-BC-2	298	2.06	16.5	−2.85	[54]
F^-CES	298	92.34	315.91	−1.85	[60]
Phenol-CES1	303	−27.23	−80	−34.6	[62]
Phenol-CEMemb	303	−39.95	−100	−27.8	[62]
Phenol-CES	303	−22.23	−70	−25.0	[62]
MB-SF/ESP composite	298	80.36	36.72	−11.3	[63]
EBT-SF/ESP composite	298	72.39	33.12	−9.7	[63]
AN57-TiO_2/CES	298	−0.11	−300	15.4	[64]
Zn^{2+}-ESP	298	27.61	143.02	−14.3	[67]
CR-ESP	293	−7.4	−21.31	−1.1	[71]
CR-CES	293	−8.84	−5.92	−7.08	[71]
CR-MWCNTs/CES	293	−17.74	−22.22	−11.4	[71]
Cr^{3+}-ESP	298	121.35	423.1	−5.7	[114]

Table 7. Conventional adsorbents used to remove selected ionic and dye pollutants.

Pollutant Ions and Dyes	Conventional Adsorbents	q_e (mg/g)	Ref.
MB dye	Tea activated carbon (TAC)	24.9–433	[115]
	Coconut shell-derived hydrochar	187.7	[116]
RBV 5 dye	Sawdust-based AC	453.0	[117]
	Coal-based AC	201.1	[117]
	Cocoa pod husk-based AC	13.0	[118]
Methyl red dye	Sepiolite	70.8	[119]
	AC	78.3	[119]
Reactive yellow dye	Rice husk AC	5000	[120]
CR dye	Carbon nanotubes	500	[121]
	Activated carbon (AC)	312.5	[121]
	Guava peel activated carbon	120.6	[122]
	Commercial activated carbon (CAC)	71.4	[123]
RhB dye	Geopolymer coal gangue	0.77–1.0	[124]
	Activated sugar-based carbon	123.5	[125]
	Activated carbon from Gmelina aborea leaves	1000	[118]
Cu^{2+}	chitosan–montmorillonite composite aerogel	87.0	[126]
	Diphenylcarbazide chitosan hydrogel	185.5	[127]

Table 7. *Cont.*

Pollutant Ions and Dyes	Conventional Adsorbents	q_e (mg/g)	Ref.
Pb^{2+}	Natural zeolite	33.9	[128]
	Sugar cane/Organge biochar	87.0/27.9	[94]
Cd^{2+}	Zeolite molecular sieves	197.5	[129]
	Natural (clinoptilolite) zeolites	15.8	[130]
	MWCNTs	201	[114]
Fe^{3+}	Natural (clinoptilolite) zeolites	17.8	[130]
Zn^{2+}	Natural zeolite	29.0	[128]
	CNTs	156.3	[131]
Ni^{2+}	Natural zeolite	27.1	[128]
	Natural (clinoptilolite) zeolites	13.1	[130]
PO_4^{3-}	Granular ternary agrowaste adsorbent	9–30	[16]
	Zr/chitosan beads	67.7	[132]
	Peanut shell biochar	3.8	[133]
	Fe/AC	6.59–15.9	[134]
	Crawfish char	9.5-70.9	[135]
SO_4^{2-}	Granular agrowaste adsorbent Granular ternary agrowaste adsorbent	77–117 22–20	[136] [137]
	Magnetic MWCNTs	56.9	[138]
	Barium-modified analcime	13.7	[139]
F^-	Activated alumina	10.2–101	[140]
	Palm shell AC, PSAC, PSAC/$MgSiO_3$	106.4 113.6	[141]
	Alumina	513.9	[142]
NO_3^-	AC from sugar beet bagasse	9.14–27.6	[143]
	GAC from grape wood	37.5	[144]
	Zero valent iron nano particles (NZVI)	36.3	[144]
	GAC/NZVI	55.8	[144]
	Carbon/silica composite	11.5	[145]
	Zr/chitosan beads	80.2	[132]

3.4. Adsorption Mechanism

Various processes and reaction mechanisms that are generally involved in adsorption of solute species (adsorbates) onto a typical eggshell particle adsorbent are illustrated in Figure 8, where the nature of the interaction depends on the functionality of the adsorbent–adsorbate system.

The three major proposed mechanisms for the adsorption of dyes and organic pollutants from the literature survey include electrostatic interactions, electrical double layer effects and interactions by weak forces involving sharing or exchange of electrons. The mechanisms of the adsorption processes are listed in Table 8, whereas Figure 8 depicts some of the contributing factors to the mechanism involved in adsorption process of pollutants onto the surface of the ESP biocomposites.

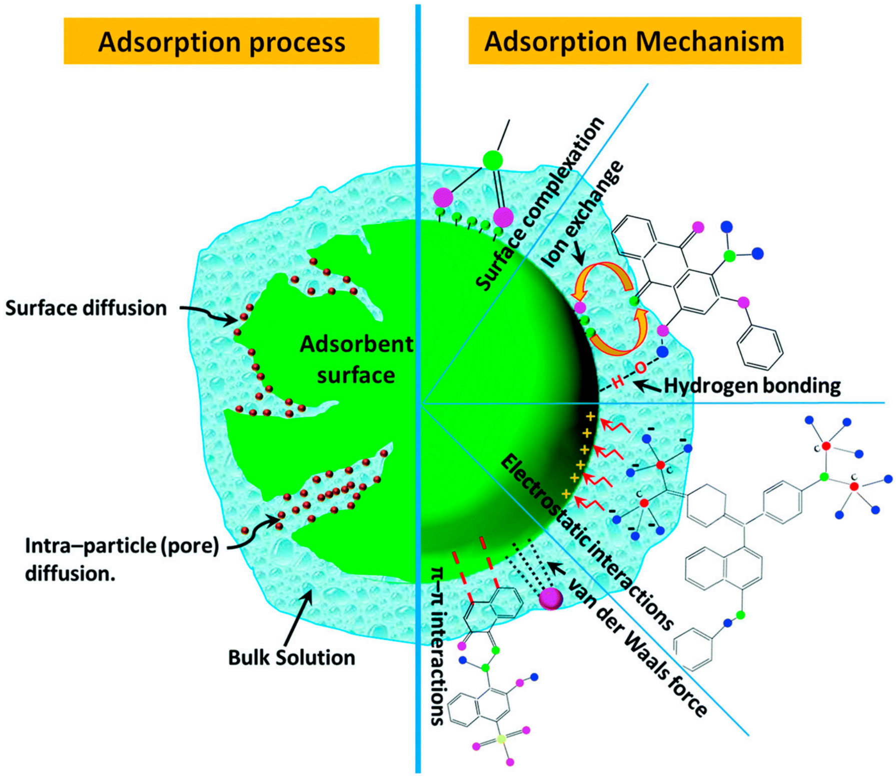

Figure 8. Contributing factors for the adsorption mechanism of pollutants onto eggshell particles. Copied with permission [146].

The adsorption of metal ions by ESP is expected to be through electrostatic interaction and/or ion exchange process because Ca^{2+} originating from eggshell particles undergoes a displacement reaction when $CaCO_3$ of the ESP was mixed with the aqueous solution [35]. The calcium salt may partially dissolve and release Ca^{2+}, and other negatively charged ions, such as CO_3^{2-}, HCO_3^{2-}, and OH^-, on the eggshell surface that can undergo exchange with other metal ions from the bulk solvent. Thus, the positively charged ions in the surrounding media were adsorbed onto the negatively charged carbonate ion on the ES surface by replacement of the dissociated calcium ions in an ion exchange process.

Further interaction for this composite adsorbent involved the adsorption of egg white protein onto the ES–metal adsorbent system. This could be due to strong and cooperative electrostatic interaction between the positively charged eggshell–metal complex and the negatively charged macromolecular proteins. The formation of a metal chelate complex with the adsorbent and protein has contributed to protein binding to metal ions by exposing electron donating amino acid residues (e.g., imidazole group) of the protein surface. The adsorption mechanism proposed for adsorption of dyes onto the eggshell–metal–egg white waste may occur via dipole interactions, and/or charge–charge interactions, but electrostatic interactions may have significant contributions.

The dye adsorption mechanism of the process for AN57 could be through electrostatic interaction of the -SO_3^- group and localized AN57 dye with the positively charged titanium and calcium ions or the partial charge of the surface oxygen bridges containing titanium and calcium oxides that attract the aromatic rings of the dye [64]. The mechanism may involve electrostatic interactions by attraction between the oppositely charged surfaces at different pH conditions [50]. Considering isotherm contribution, chemisorption is the feasible mechanism for the process to occur and was supported from the fitting results of the kinetic models. The PSO model provided the best-fit results for the data, which also supports chemisorption. An adsorption mechanism was proposed for the removal of EBT and MB, where electrostatic attraction between the negative adsorbents and positive MB occur at basic pH, whereas positive adsorbents and negative EBT dye occur at acidic pH, which is largely controlled by chemisorption [63].

A mechanism was reported [7] for the sorption process that may involve valence forces through sharing or exchange of electrons between sorbent and sorbate, that is between MB/CEAC [147], which could involve exchangeable H^+ ions with the SiO-H or OH groups. A study of the adsorption of MB dye onto the eggshell sorbent reported that electrical double layer effects maintain surface neutrality of the adsorbent, and provide an account of the adsorption process [48]. The pores between the collagen and glycoprotein fibers of the ES membrane contributed to the movement of ions and calcium salts in the ES to dissolve when mixed with the dye solution to release Ca^{2+}, HCO_3^-, CO_3^{2-}, and OH^-· [41,148,149]. The process of ion transport via the ES pores may play a key role in the released ions adsorbed onto the eggshell surfaces that form negative ions [48]. The solution also contains some cations such as Na^+, Mg^{2+}, and K^+, which may be adsorbed onto the surface of the ES and form an electrical double layer, where the ES surface acquires a positive charge [48]. In this way, ions from the solution can be adsorbed onto the negatively charged membrane surface. The adsorption mechanism proposed for the CR dye was attributed to electrostatic interactions between the -SO_3^- group of the dye and the positive surface charge of the ES, especially at low pH.

Electrostatic interaction and /or cation exchange is responsible for the adsorption of Zn^{2+} onto ESP and the negatively charged ions, such as CO_3^{2-}, HCO_3^-, OH^-, and cation exchange with Ca^{2+} and Zn^{2+}. BSA adsorption onto the composite may occur through combined effects involving electrostatic interactions between the positively charge biocomposite and the negatively charged BSA and/or metal–chelate interactions via electron-donating amino acids of BSA with the ESP/Zn composite [67].

Various ES biocomposites display efficient adsorption to a wide variety of dyes from cationic to basic at variable pH, where remazol dye and RY 145 sits at acidic pH 2, CR and MB at neutral pH 7, and TB at pH 12. This showed that the ES biocomposites enable treatment of a wide range of wastewater systems for the removal of pollutants.

Several mechanisms that account for the removal of metal ions by adsorbents are metal complexation, electrostatic attraction, ion exchange, and precipitation. The ion exchange mechanism seemed to be generally involved for the adsorption of metal ions onto ESP or its composites. A list of contributions to the adsorption mechanism are listed in Table 9.

Chemical and electrostatic interactions, precipitation, and hydrogen bonding contribute to the probable mechanisms for the adsorption of anions onto the various ES biocomposites. Chemical precipitation and electrostatic interactions between the calcite surface (from ESP) and the fluoride ions is a possible mechanism for the removal of fluoride from wastewater. The key ions in a pure calcite solution are Ca^{2+} and CO_3^{2-}, which also occur along any cleavage site on the calcite surface, where these ions possess unsatisfied partial charges. In aqueous solution, these ions can easily react with other ions that are present in the medium [23,43,56,57]. The removal mechanism for nitrate is chemisorption and redox reaction, where the identification of new bands after the adsorption experiment showed that a new chemical species, ferric nitrate ($Fe(NO_3)_3 \cdot 9H_2O$), was formed by chemisorption through covalent bonding and iron oxide (FeO) was formed by a redox reaction [42]. Ion exchange is another probable mechanism for the adsorption of phosphorus onto aluminum compounds that contain hydroxyl groups [44].

The preceding section outlined the adsorption of cationic pollutants onto the ESP biocomposites with an emphasis on metal ions and the potential type of mechanism involved in the process. Similarly, the adsorption of anionic pollutants allows for conclusions based on our observations. Chemical and electrostatic interactions, precipitation, and hydrogen bonding are the main contributions that account for the adsorption process. For the case of cationic pollutants, similar contributions to the adsorption mechanism were described.

Table 8. Mechanism of the adsorption process of dyes molecules onto ESP/biocomposites.

Mechanism	Pollutant/Adsorbent	Remarks and Reference
Electrostatic Interaction (EI)	AN57 dye/CES-TiO_2, Styryl pyridinium tailored dye/ESP-SDS, Reactive yellow 145 dye/ESP and Cd^{2+}/CES CR/ESP MB/Immob ESP and EBT/Immob ESP Zn/ESP; BSA/ESP/Zn MB/CEAC Remazol reactive red 198 dye/Immob ESP with PVC and alginate CR/CES RBV-5R/ES MB/ESP	Interaction of -SO_3^- and localized dye with Ti^{2+} or Ca^{2+} [64]. Ionic bond formation between sulphate groups and the cationic amino acid side chains of the tailored dye due to oppositely charged surfaces at variable pH [20]. Result obtained from point of zero charge allowed a suitable control of pollutant pH and thus electrostatic attraction was attributed to their adsorption [50]. Electrostatic interactions between -SO_3^{2-} of the dye and the eggshell whose surface is positively charged at low pH is responsible for the mechanism [48]. Electrostatic attraction between oppositely charged ions at different pH [63,67]. Interaction of adsorbate with surface CaO, SiO_2, Al_2O_3, and ZrO_2 sites on the CEAC [49]. Kinetic results support the role of chemisorption and exchangeable H^+ present at the -SiOH or -OH groups of eggshell could interact with the adsorbate [7]. The zeta potential (+10 mV) is suggestive of electrostatic interactions [71]. The dye sulfonate group is attracted to the protonated ES surface [53]. Pores between the collagen and glycoprotein fibers in the eggshell membrane-controlled movement of ions and dissolution of calcium salt of the eggshell, where the dye in solution leads to the release of ions as a major contributor to this mechanism [48].
Involves weak valence forces and sharing or exchange of electrons	CR/MWCNTs-CES	Adsorption via van der Waals forces is proposed. Negative zeta potential suggests electrostatic repulsive forces, where weak intermolecular forces play an important role [71].

Table 9. Mechanism involved in the adsorption of metal ions onto ESP biocomposites.

Mechanism	Pollutant/Adsorbate	Ref.
Ion exchange: Ion exchange occurred between metal ions and Ca^{2+} on the eggshell surface or onto $CaCO_3$ $M^{2+}_{(solution)} + Ca^{2+}_{(adsorbent)} \rightleftharpoons M^{2+}_{(adsorbent)} + Ca^{2+}_{(solution)}$	Ni^{2+}, Cu^{2+}, Cd^{2+}/WM, ESP, ESH-M Pb/ESP; Na-ESP; HN-ESP; K-ESP Mechanically activated $CaCO_3$/MSO_4 AMD/Bentonite, ESP, BEP Pb/CHAP Al^{3+}, Fe^{2+}, Zn^{2+}/ESP Cd^{2+}, Cu^{2+}, Pb^{2+} and Zn^{2+}/Ch, SBFL, ESP, HK	[67,110] [41] [38] [39] [36] [106] [107]
Precipitation: Precipitation can occur since adsorption is pH dependent. If pH is high, precipitation can take place resulting in the formation of hydroxides or carbonates. $CaCO_3 \rightleftharpoons Ca^{2+} + CO_3^{2-}$ $CO_3^{2-} + H_2O \rightleftharpoons HCO_3^- + OH^-$	Al^{3+}, Fe^{2+}, Zn^{2+}/ESP Mechanically activated $CaCO_3$/MSO_4 Cd^{2+}, Cu^{2+}, Pb^{2+} and Zn^{2+}/Ch, SBFL, ESP, HK	[106] [73] [107]
Electrostatic attraction: Occurs between oppositely charged ions.	Ni^{2+}, Cu^{2+}, Cd^{2+}/WM, ESP, ESH, ESP-M Pb^{2+}/ESP; Na-ESP; HN-ESP; K-ESP Pb from AMD/Bentonite, ESP, BEP	[67,110] [41] [39]
Metal complexation: It may involve complexation of OH^- or CO_3^{2-} between Pb^{2+} and ligands on the adsorbent surface.	Pb^{2+}/ESP; Na-ESP; HN-ESP; K-ESP Pb^{2+} from AMD/Bentonite, ESP, BEP Pb^{2+}/CHAP	[41] [39] [36]

From a survey of the literature, the mechanisms governing the adsorption of inorganic cation and anion pollutants with ESP, or its composites involve similar contributions. A major contribution for ESP binding relates to the release of charged particles from the adsorbent surface.

4. Future Perspectives

The sustainability of ES composites is an issue with considerable relevance to various industries (Figure 9). Sustainability could be viewed from different perspectives such as cost, environmentally benign materials, feedstock abundance, and renewability of the raw materials. Table 10 provides an overview of various applications that utilize ESP in various fields of application, which contribute to sustainability. The utilization of ES waste for various applications apart from its use as adsorbent materials for pollutant removal are Mallakpour et al. [150]. This includes cement formulation production, dressings for burns, cosmetics, substrates for cell culture, templates for forming ordered tube networks [151], catalyst supports for immobilization of enzymes and ES-reinforced polymer composites.

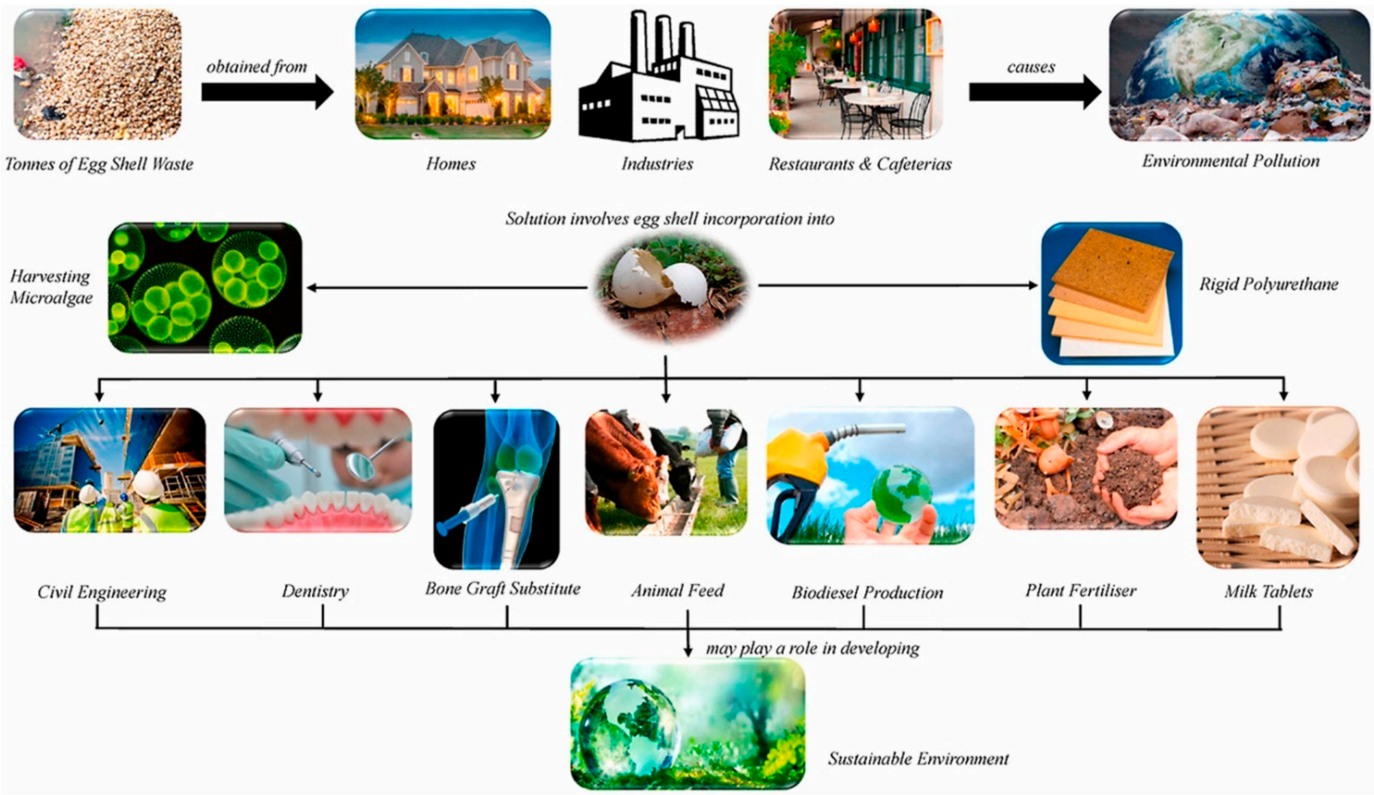

Figure 9. Application of eggshell in various industries. Copied with permission [74].

Table 10. Utilization of ESP in different fields of application.

Application	Reference
Thermosetting composite blends	[152,153]
Catalyst for biodiesel production	[154]
Organic fertilizer	[155]
Milk tablet supplement	[156]
Adsorbent for carbon dioxide	[74]
Pharmaceutical formulations for controlled-release	[157]
Pigment coatings	[158]
Lithium-sulphur batteries	[159]

Table 10. *Cont.*

Application	Reference
Lactose free milk	[160]
Harvesting certain microalgae	[161]
Supplement in animal feed	[162]
Stabilization of lateritic soils for construction materials	[163]
Metal matrix composites and friction materials	[164]
Thermoplastic composite fillers	[25]
Bone mineralization	[25,165]
High temperature carbon monoxide capture	[153,166–169]
Adsorption based-removal of insecticides in beverage samples	[166]
Solvent assisted solid phase extraction of PAHs	[170]
Adsorptive removal of non-radioactive strontium from aqueous solutions	[171]
Removal of divalent metal ions e.g., cadmium, lead	[37,150]
Adsorptive removal of organics (neutral red, bromocresol green and tetracycline HCl)	[172]
Application to solar thermochemical energy storage	[173]
Sorption of dyes	[174]
Separation and magnetic extraction of superparamagnetic composite materials	[175]
Dichlorination and liquefaction of mixed plastics containing PVC	[176]
Dehalogenation: removal of Br^- and Cl^-	[176]
HCl gas capture via adsorption	[177]
Desulphurization of dibenzothiophene	[178]
Recovery of F^- from wastewater	[9]

ES composites are employed in pharmaceutical applications, such as for bone mineralization and growth in animals and in humans and for calcium deficiency therapies. As well, ES powder was used in maxillofacial surgery as a bone substitute, where ES powder is reported to reduce pain and increase bone density [25].

ES composite blends also find utility as fillers, where it was reported that blends of thermoplastic/eggshell composites enhanced various properties, such as lower density, higher crystallinity, good mechanical properties (tensile strength and Young's modulus), and high thermal resistance. A higher Young's modulus was observed in polypropylene blended with 40% ES filler as compared to that with similar quantity of abiogenic (mineral-based) $CaCO_3$ [179]. Similarly, improved properties such as higher crystallinity and lower density were obtained in PP blends with ES, in comparison with a mineral calcium carbonate mineral [25]. The corresponding PP composites can be applied in lightweight and low load-bearing applications [25]. Investigation on the properties of composite foams with cornstarch and ES revealed that with 0 to 6% ES filler, certain properties decreased, such as expansion ratio, foam unit density, and foam cell size, while others, like spring index, reveal an increase [180].

The utility of ES was not limited to thermoplastic composites alone, but also extends to thermoset composites, which were incorporated with epoxy resin to improve its mechanical toughness [181]. The morphology of the polymer, poly (styrene-ethylene-styrene) blended with ES showed good dispersion and minimum large voids [182]. Incorporation of ES as filler in natural rubber [152] revealed that the elastomer polymer composite had the highest tensile strength, swelling resistance, tear strength, and hardness compared to other fillers. In addition, it was reported that natural rubber mixed with ES filler has similar properties as a flame retardant and curing agent, with those made from conventional calcium carbonate [183]. As well, natural rubber with ES filler had similar tensile strength in comparison to those mixed with mineral $CaCO_3$ [153].

ES particles were used as low-cost catalysts in chemical transformations and organic synthesis, along with the production of biodiesel by the transesterification of vegetable oils with methanol [184–186]. Although ES was applied to agricultural soil to increase soil pH, ES was also used as a stabilizing agent for clay-related components, where it is used to stabilize lateritic soils for construction materials [163]. In turn, ES addition can also improve soil quality by reducing the plastic indices of soil samples.

A key sustainability goal is to develop unique types of ESP-based composites for potential replacement of abiogenic $CaCO_3$ (derived from limestone) with biogenic systems derived from ES for various products, especially where calcite mineral is required. Biogenic alternatives will serve to address waste disposal by valorization of eggshells and offset the cost of mining, production, and preservation of the physical environment due to potential disruptive activities relevant to mining operations. An area of interest in the scientific literature that is under-reported relates to green disposal techniques for 'spent' ESP adsorbents. Much of the research reported relates to laboratory scale studies, where the use of ESP biocomposite adsorbents at the pilot scale is recommended as an area of future work. Pilot scale studies apply to real industrial wastewater treatment in a dynamic process versus simulated "laboratory" wastewater, along with techno-economic analysis of ESP. Since various reports indicate that CES outperformed ESP, the diversion of eggshell waste from landfills can potentially reduce harmful leachate from landfills to other material platforms for other value-added products (e.g., preparation of calcium phosphate bioceramics such as hydroxyapatite) [187].

Based on the results presented for various types of ESP composite adsorbents, it can be concluded that the adsorption properties toward a range of pollutants (dyes, organics, and ionic species) reveal variable levels of removal efficiency. While these results were focused mainly on single component adsorbate systems, there is a need to explore other aspects of adsorption science and technology for ESP composite adsorbents as part of future perspectives in the field. This includes the study of multicomponent adsorbate systems, due to the role of potential competitor effects in complex matrices, such as environmental samples and industrial wastewater systems. Additionally, adsorption studies of multicomponent systems can be evaluated to explore the role of adsorption-based selectivity. The use of computational methods such as density functional theory (DFT) and equilibrium surface complexation models (SCMs) can be investigated to gain insight on competitive adsorption at available binding sites. In this way, the use of computational methods can be employed to gain further insight on the role of ESP as an additive in composite adsorbent materials, which will contribute to future efforts in their rationale design. To establish the sustainability of ESP composite adsorbents, there is a need to evaluate potential limitations of ESP related to its processing, and step-wise processes, such as grinding, membrane removal, and calcination temperature to establish ESP with suitable physicochemical properties. In the context of ESP composites preparation, the optimization of the ESP content (and other additives) during synthesis to obtain suitable mechanical properties and adsorption properties of the composite is recommended. The design of improved mechanical properties for ESP biocomposites is anticipated to contribute to adsorbents with improved recyclability over multiple adsorption-desorption cycles, as described above. Techno-economic analysis of ESP-biocomposite adsorbents should be carried out, along with a comparison of currently available commercial biocomposite adsorbents to evaluate their overall sustainability. In turn, research along these lines can serve to address the development of various composite adsorbents with improved adsorption properties for diverse applications. Section 4.1 provides an overview of several case studies of ESP composites for selected adsorption-based applications. These examples provide the motivation to develop such systems with improved properties for diverse applications as catalysts, carrier systems, and adsorbents for innovative water treatment technology.

4.1. Eggshell Waste in Catalytic Applications

The use of eggshell as catalyst systems are outlined across four categories, as illustrated in Figure 10:

(1) Biodiesel production: The search for biodiesel as alternatives to conventional fossil fuels is supported by the increasing rise of global warming and energy crises. Biodiesels are produced by transesterification of triglycerides with methanol using catalysts at various conditions (reaction time, type and ratio of starting material, and catalyst loading), but it is reported that the role the calcium oxide content and catalyst surface area are very important in catalytic activity. A commonly used heterogeneous catalyst is CaO, which can be obtained from different sources such as eggshell or ashes [167]. It was reported that 95% biodiesel yield was obtained when the calcination of ES is performed above 800 °C [188], while a yield of 90% and reusability of the catalyst up to six times without significant loss in activity [123]. In 2010, investigation on the use of quail and chicken eggshell for the production of biodiesel and the quail eggshell was reported to provide better catalytic activity [189]. Another study reported a yield of 100% biodiesel from used cooking oil [190].

(2) Hydrogen gas synthesis: A cleaner alternative fuel that yields less pollution is desirable because CO_2 is a major greenhouse gas released through anthropogenic activities. Thus, H_2 is receiving greater attention and its production through gasification is a research topic of interest. Gasification of carbonaceous material can be significantly improved using catalyst [191]. The addition of eggshell as catalyst suppressed the production of CO_2, due to adsorption by CaO, which also promotes H_2 generation by the water gas shift reaction [192].

(3) Industrial chemical production: Less toxic chemicals such as dimethyl carbonate, oximes, and glycerol oligomers used in the methylation reaction and other organic synthesis are replacing the more toxic ones like dimethyl halides and dimethyl sulfate. Successful dimethyl carbonate synthesis was performed using calcined eggshell as the catalyst. Transesterification of propylene carbonate and methanol was done, where 75% DMC yield was obtained. It was reported that ESP showed similar activity to pure CaO.

(4) Synthesis of bioactive compounds: Bioactive compounds are used in cosmetics, pigments, and biodegradable agrochemicals. The use of catalysts based on eggshell to synthesize bioactive compounds like chromenes, pyran derivatives, and aromatic aldehydes were reported previously. ES have been used in the synthesis of 2-aminochromenes and pyrano[4,3-b]pyrans. These compounds possess antiviral, anticarcinogenic, and antifungal activities [193,194].

The utility of eggshells in photodegradation of organic pollutants such as dyes share features that are important in various aspects of catalysis, such as the key role of adsorption in the case of photocatalytic degradation of dye. The photodegradation process is illustrated in Figure 11 for methylene blue and toluidine blue, which involves the role of dye adsorption onto calcium oxide derived from ES waste. The role of adsorption-based processes are further revealed in Section 4.2.

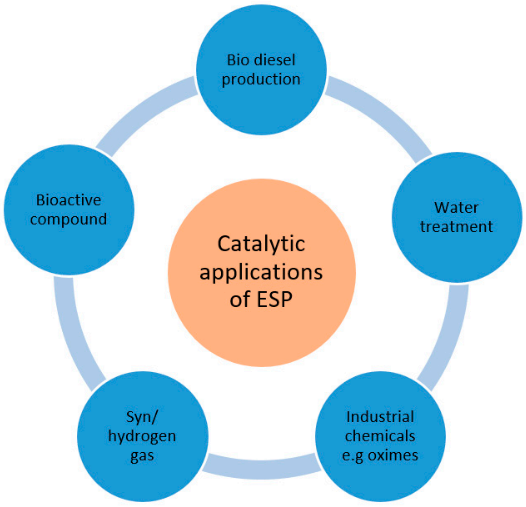

Figure 10. Application of eggshell waste in catalysis.

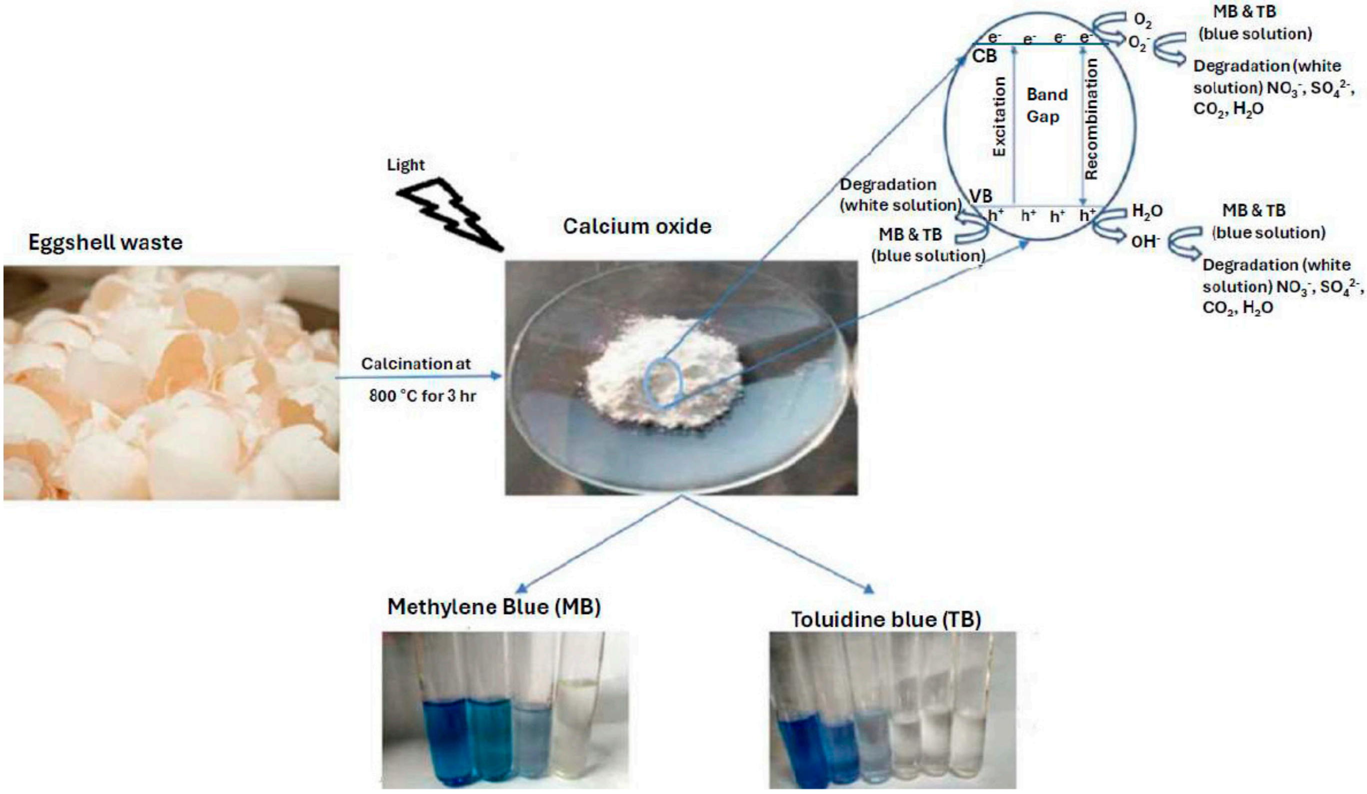

Figure 11. Application of ES as a photocatalyst in water treatment. Copied and redrawn with permission [59].

4.2. The Use of Eggshell Waste in Slow-Release Fertilizer (SRF) System

The ability to provide a continuous supply of fertilizer for ensuring good crop yield is necessary to meet the demands for addressing food security for the world's growing population. In the case of non-uniform application of fertilizer, inefficiency in fertilizer uptake by plants are known as a source of pollution to land, air, and water due to vaporization into the atmosphere, leaching, and surface run-off. In a bid to circumvent the various limitations and challenges faced in the controlled application of fertilizer to agricultural fields, slow-release delivery systems have the potential to enable more efficient, cost-effective, and sustainable uptake of fertilizer. The potential utility of ES-based substrates as a viable support for SRF was reported by Dayanidhi et al. [195], where the ES-SRF system and its preparation are outlined in Figure 12.

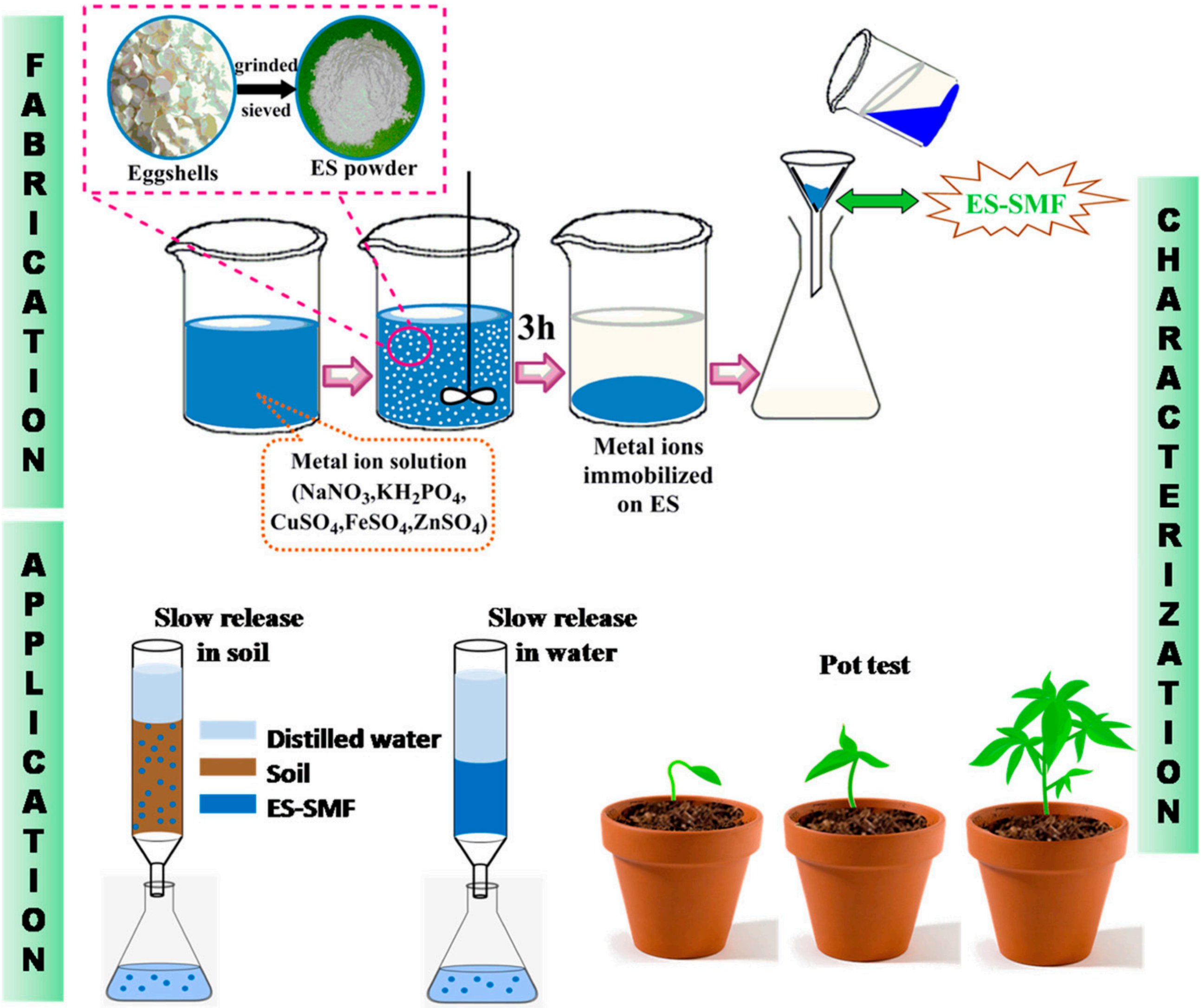

Figure 12. Application of eggshell as a slow-release fertilizer system. Adapted with permission [195].

In this work, an investigation of the use of ES as a support to supplement nutrients in soils was reported, where soils with ES-SRF had greater plant growth (height and root length) when compared to the soils treated with pristine ES or without any treatment (ES or ES-SRF). The germination rate of the tested crops, i.e., cucumber and tomato, increased by 57.7 and 76.0%, respectively; moreover, the application of ES-SRF led to improved water holding and water retention capacities of the soils (cf. Figure 13). It was inferred that ES-SRF serves as a reservoir of nutrients that was capable of providing essential nutrients to plants throughout the growth period.

The production of $K_3CaH(PO_4)_2$ and $CaKPO_4$ was reported by using a mechanochemical process between eggshell and KH_2PO_4 [196]. There is a better management of P, K, and Ca when the produced $K_3CaH(PO_4)_2$ and $CaKPO_4$ are applied to soil systems. The result showed an increase in phosphorous (P) release from 0 to 25 mg/kg after 3 days and 45 mg/kg at 30 days, indicating that a longer delay in P release was realized.

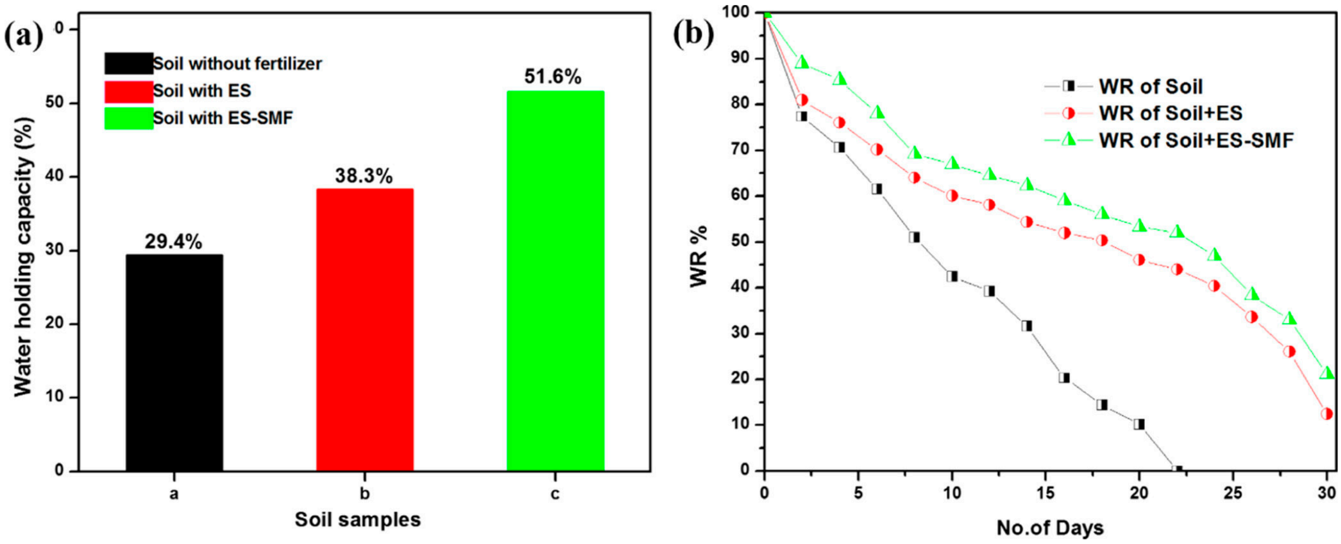

Figure 13. (**a**) Water holding capacity and (**b**) water retention capacity of soil with and without ES and ES-SRF. Copied and modified with permission [195].

As shown in Figure 14, a granular adsorbent made from torrefied wheat straw, eggshells, and chitosan was used for orthophosphate adsorption studies, where the results revealed that the granular adsorbent was capable of adsorbing 23–30 mg/g orthophosphate at pH 4.5, and between 9–12 mg/g at pH 8.5 [16]. This study highlights the role of closed loop-processes, where one loop for the design of a suitable adsorbent from waste biomass (e.g., ESP and wheat straw); whereas a second loop demonstrates the utility of adsorbed phosphate as a SRF system can be applied for agricultural crop production.

The utilization of ES substrate for the preparation of composite adsorbents represents a target material for the valorization and utilization of ES waste. The utility of ES-based materials is further illustrated in their application for the removal of pollutants from wastewater, as described in Section 4.3.

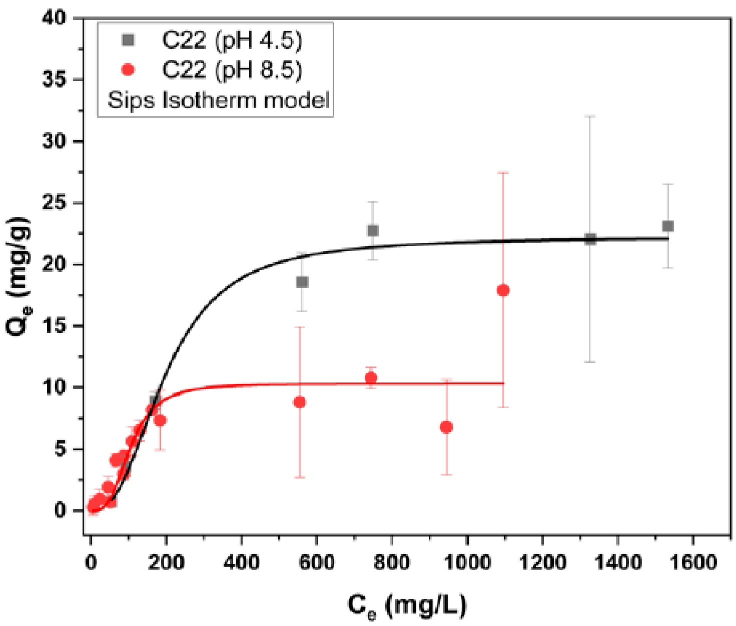

Figure 14. The use of granular ternary agro-waste adsorbent for orthophosphate uptake at pH 4.5 and 8.5. Copied with permission [16].

4.3. Eggshell Applications in Wastewater Treatment

The review is devoted to the use of ESP biocomposites as adsorbents for the removal of various pollutants from water, along with other applications illustrated in Figure 9. In Figure 15, an illustrated view of the preparation and utilization of the ES adsorbent for metal-ion removal and recovery is outlined.

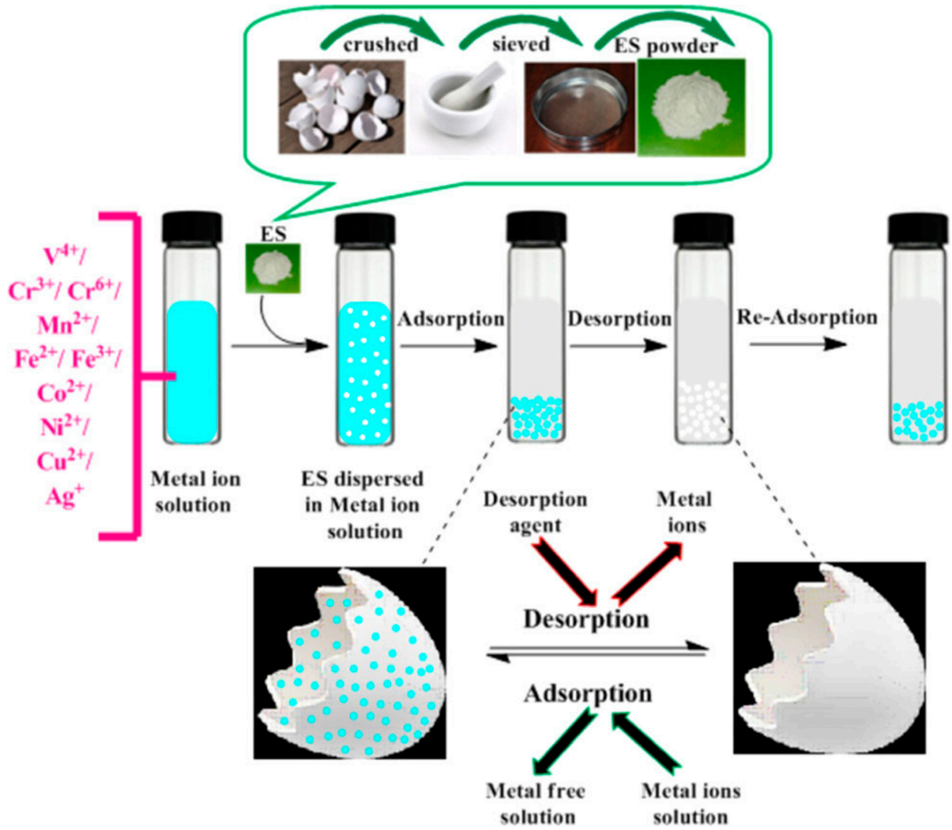

Figure 15. Application of eggshell in treatment of water containing metal-ion species. Copied with permission [197].

5. Conclusions

This review provides a summary of studies related to the preparation and utilization of ES composites over the last decade. This includes the ES pretreatment, preparation of composites, and characterization of the adsorption properties of ES composites at equilibrium and kinetic conditions. This overview is unique since many review articles that discuss ES particles focus largely on two types of general applications of value-added products: (i) industrial applications as structural composites in polymer, metal matrix, additives, and catalysts in biodiesel production and (ii) medical applications for utility in dentistry and orthopedics, food, and drug supplements. Various results for the adsorption of pollutants (dyes, insecticides, metal ions, anions, and oxyanions) that employ ESP biocomposites over the last decade was presented. The equilibrium isotherms and thermodynamic and kinetic parameters reported for the effective removal of various pollutants reveal the utility and feasibility of various ES adsorbents. In general, ES composite adsorbents generally display enhanced adsorption properties over ES materials in their pristine form or ES particles that are modified by chemical or thermal treatment (by calcination or pyrolysis). Pretreatment of ES was generally done by washing, oven-drying, grinding, and sieving, while final preparations involved mixing certain quantities of additives (inorganic to organic) to afford formation of ES composites via physical blending to yield products with variable composition with tailored properties.

CES was reported to be more efficient in the removal of pollutants due to increased surface area and pore sizes; the characterization revealed that calcite is present in ESP biocomposite as the dominant polymorph of calcium carbonate that is often employed in many industrial applications. A major influence on the role played by ESP relates to the release of charged particles on the surface of the biosorbents via ion-exchange. The adsorption mechanism of organic and inorganic pollutant removal with eggshell powder and its composites can be physisorption or chemisorption. This includes chemical and electrostatic interactions, precipitation, and hydrogen bonding, metal complexation, ion exchange, electric double layer effects, and weak valence forces leading to sharing or exchange of electrons. Usage of ESP biocomposites allow the modification of the physicochemical properties of the multicomponent systems to achieve composites that can be developed further for applications with tailored physicochemical properties.

The importance of developing such composites is attributed to their end-use applications (Table 10). We anticipate that this review will inspire further research on ES utilization for the development of composite materials to address a number of global challenges: (i) sustainability challenges for the diversion of ES waste, (ii) the valorization and utilization of ES waste, and (iii) the end-use applications with an emphasis on adsorbent technology for adsorption-based processes (slow fertilizer release, environmental remediation, chemical separations, catalytic processes, etc.). Adsorption science and technology holds the promise of addressing controlled removal of pollutants that serve to address water security to address environmental remediation and concerns related to the health of ecosystems and human health. In turn, ESP biocomposite adsorbents are envisaged to have broad appeal across many sectors of industry and technological processes, such as remediation of chemical pollutants in industrial wastewater and advanced drinking water treatment processes. This review highlights the importance of utilization and valorization of ES waste from a sustainability perspective, which will promote a circular economy design strategy via recycling of an abundant source of biogenic calcite. Additionally, the successful utilization of ES biocomposites as adsorbents will contribute to the UN SDGs; namely, water and sanitation (SDG 6), industry, innovation and infrastructure (SDG 9), and waste reduction, recycling, and reuse (SDG-12) [16].

Supplementary Materials: The following supporting information can be downloaded at: https://www.mdpi.com/article/10.3390/jcs8100414/s1, Section S1: Equilibrium Isotherm Models; Section S2: Kinetic models; Table S1: Adsorption Isotherm models and parameters; Table S2: Adsorption kinetic models and parameters.

Author Contributions: Conceptualization, L.D.W.; methodology, B.M.B.; validation, L.D.W. and B.M.B.; formal analysis, B.M.B.; investigation, B.M.B.; resources, L.D.W.; data curation, B.M.B.; writing—original draft preparation, B.M.B.; writing—review and editing, L.D.W. and B.M.B.; visualization, L.D.W. and B.M.B.; supervision, L.D.W.; project administration, L.D.W.; funding acquisition, L.D.W. All authors have read and agreed to the published version of the manuscript.

Funding: This research was funded by the Government of Canada through the Natural Sciences and Engineering Research Council in the form of a Discovery Grant (RGPIN 04315-2021) to L.D.W. B.M.B. acknowledges fellowship support (TETF/ES/UNIV/EKITI STATE/TSAS/2021) received from Tertiary Education Trust Fund (TETFund) Nigeria for postdoctoral studies at the University of Saskatchewan.

Data Availability Statement: No new data were created in this study, data sharing is not applicable.

Acknowledgments: The authors wish to make a land acknowledgement that this work was carried out in Treaty 6 Territory and the Homeland of the Métis. As such, we pay our respect to the First Nations and Métis ancestors of this place and reaffirm our relationship with one another.

Conflicts of Interest: The authors declare no conflicts of interest.

References

1. Gasper, D.; Shah, A.; Tankha, S. The Framing of Sustainable Consumption and Production in SDG 12. *Glob. Policy* **2019**, *10*, 83–95. [CrossRef]
2. Vandeginste, V. Food waste eggshell valorization through development of new composites: A review. *Sustain. Mater. Technol.* **2021**, *29*, e00317. [CrossRef]
3. Lee, M.; Tsai, W.-S.; Chen, S.-T. Reusing shell waste as a soil conditioner alternative? A comparative study of eggshell and oyster shell using a life cycle assessment approach. *J. Clean. Prod.* **2020**, *265*, 121845. [CrossRef]
4. Zhang, X.; He, X.; Kang, Z.; Cui, M.; Yang, D.-P.; Luque, R. Waste Eggshell-Derived Dual-Functional CuO/ZnO/Eggshell Nanocomposites: (Photo)catalytic Reduction and Bacterial Inactivation. *ACS Sustain. Chem. Eng.* **2019**, *7*, 15762–15771. [CrossRef]
5. Pliya, P.; Cree, D. Limestone derived eggshell powder as a replacement in Portland cement mortar. *Constr. Build. Mater.* **2015**, *95*, 1–9. [CrossRef]
6. Homavand, A.; Cree, D.E.; Wilson, L.D. Polylactic Acid Composites Reinforced with Eggshell/$CaCO_3$ Filler Particles: A Review. *Waste* **2024**, *2*, 169–185. [CrossRef]
7. Elkady, M.; Ibrahim, A.M.; El-Latif, M.A. Assessment of the adsorption kinetics, equilibrium and thermodynamic for the potential removal of reactive red dye using eggshell biocomposite beads. *Desalination* **2011**, *278*, 412–423. [CrossRef]
8. De Angelis, G.; Medeghini, L.; Conte, A.M.; Mignardi, S. Recycling of eggshell waste into low-cost adsorbent for Ni removal from wastewater. *J. Clean. Prod.* **2017**, *164*, 1497–1506. [CrossRef]
9. Chen, W.; Wu, Y.; Xie, Z.; Li, Y.; Tang, W.; Yu, J. Calcium hydroxide recycled from waste eggshell resources for the effective recovery of fluoride from wastewater. *RSC Adv.* **2022**, *12*, 28264–28278. [CrossRef]
10. Gu, T.; Yin, C.; Ma, W.; Chen, G. Municipal solid waste incineration in a packed bed: A comprehensive modeling study with experimental validation. *Appl. Energy* **2019**, *247*, 127–139. [CrossRef]
11. Ramachandra, T.; Bharath, H.; Kulkarni, G.; Han, S.S. Municipal solid waste: Generation, composition and GHG emissions in Bangalore, India. *Renew. Sustain. Energy Rev.* **2018**, *82*, 1122–1136. [CrossRef]
12. Cudjoe, D.; Acquah, P.M. Environmental impact analysis of municipal solid waste incineration in African countries. *Chemosphere* **2021**, *265*, 129186. [CrossRef] [PubMed]
13. Sondh, S.; Upadhyay, D.S.; Patel, S.; Patel, R.N. A strategic review on Municipal Solid Waste (living solid waste) management system focusing on policies, selection criteria and techniques for waste-to-value. *J. Clean. Prod.* **2022**, *356*, 131908. [CrossRef]
14. Ferraz, E.; Gamelas, J.A.F.; Coroado, J.; Monteiro, C.; Rocha, F. Eggshell waste to produce building lime: Calcium oxide reactivity, industrial, environmental and economic implications. *Mater. Struct.* **2018**, *51*, 115. [CrossRef]
15. Zhang, X.; Chelliappan, B.; Rajeswari, S.; Antonysamy, M. Recent Advances in Applications of Bioactive Egg Compounds in Nonfood Sectors. *Front. Bioeng. Biotechnol.* **2021**, *9*, 738993. [CrossRef]
16. Steiger, B.G.K.; Bui, N.T.; Babalola, B.M.; Wilson, L.D. Eggshell incorporated agro-waste adsorbent pellets for sustainable orthophosphate capture from aqueous media. *RSC Sustain.* **2024**, *2*, 1498–1507. [CrossRef]
17. Mohamed, M.H.; Udoetok, I.A.; Solgi, M.; Steiger, B.G.K.; Zhou, Z.; Wilson, L.D. Design of Sustainable Biomaterial Composite Adsorbents for Point-of-Use Removal of Lead Ions from Water. *Front. Water* **2022**, *4*, 739492. [CrossRef]
18. Ho, W.-F.; Hsu, H.-C.; Hsu, S.-K.; Hung, C.-W.; Wu, S.-C. Calcium phosphate bioceramics synthesized from eggshell powders through a solid state reaction. *Ceram. Int.* **2013**, *39*, 6467–6473. [CrossRef]
19. Hassan, T.A.; Rangari, V.K.; Rana, R.K.; Jeelani, S. Sonochemical effect on size reduction of $CaCO_3$ nanoparticles derived from waste eggshells. *Ultrason. Sonochem.* **2013**, *20*, 1308–1315. [CrossRef]
20. Guru, P.S.; Dash, S. Adsorption of Some Tailor-Made Styrylpyridinium Dyes on Sodium Dodecylsulphate-Treated Eggshell Particles (SDS-ESP): Impact of Dye Chain-Length and Substituent. *J. Dispers. Sci. Technol.* **2013**, *34*, 898–907. [CrossRef]
21. Elwakeel, K.Z.; Yousif, A.M. Adsorption of malathion on thermally treated egg shell material. *IWTC* **2010**, *14*, 53–65. [CrossRef] [PubMed]
22. Tizo, M.S.; Blanco, L.A.V.; Cagas, A.C.Q.; Cruz, B.R.B.D.; Encoy, J.C.; Gunting, J.V.; Arazo, R.O.; Mabayo, V.I.F. Efficiency of calcium carbonate from eggshells as an adsorbent for cadmium removal in aqueous solution. *Sustain. Environ. Res.* **2018**, *28*, 326–332. [CrossRef]
23. Bhaumik, R.; Mondal, N.K.; Das, B.; Roy, P.; Pal, K.C.; Das, C.; Baneerjee, A.; Datta, J.K. Eggshell powder as an adsorbent for removal of fluoride from aqueous solution: Equilibrium, kinetic and thermodynamic studies. *J. Chem.* **2012**, *9*, 1457–1480. [CrossRef]
24. Pérez, S.; Muñoz-Saldaña, J.; Acelas, N.; Flórez, E. Phosphate removal from aqueous solutions by heat treatment of eggshell and palm fiber. *J. Environ. Chem. Eng.* **2021**, *9*, 104684. [CrossRef]
25. Guru, P.S.; Dash, S. Sorption on eggshell waste—A review on ultrastructure, biomineralization and other applications. *Adv. Colloid Interface Sci.* **2014**, *209*, 49–67. [CrossRef]
26. Owuamanam, S.; Cree, D. Progress of bio-calcium carbonate waste eggshell and seashell fillers in polymer composites: A review. *J. Compos. Sci.* **2020**, *4*, 70. [CrossRef]
27. Bashir, A.S.M.; Manusamy, Y. Characterization of Raw Egg Shell Powder (ESP) as a Good Bio-filler. *J. Eng. Res. Technol.* **2016**, *2*, 2015. Available online: https://journals.iugaza.edu.ps/index.php/JERT/article/view/1637 (accessed on 1 September 2024).
28. Nys, Y.; Gautron, J.; Garcia-Ruiz, J.M.; Hincke, M.T. Avian eggshell mineralization: Biochemical and functional characterization of matrix proteins. *C. R. Palevol* **2004**, *3*, 549–562. [CrossRef]

29. Arias, J.L.; Fink, D.J.; Xiao, S.-Q.; Heuer, A.H.; Caplan, A.I. Biomineralization and Eggshells: Cell-Mediated Acellular Compartments of Mineralized Extracellular Matrix. *Int. Rev. Cytol.* **1993**, *145*, 217–250. [CrossRef]
30. Boronat, T.; Fombuena, V.; Garcia-Sanoguera, D.; Sanchez-Nacher, L.; Balart, R. Development of a biocomposite based on green polyethylene biopolymer and eggshell. *Mater. Des.* **2015**, *68*, 177–185. [CrossRef]
31. Mittal, A.; Teotia, M.; Soni, R.; Mittal, J. Applications of egg shell and egg shell membrane as adsorbents: A review. *J. Mol. Liq.* **2016**, *223*, 376–387. [CrossRef]
32. Ketta, M.; Tůmová, E. Eggshell structure, measurements, and quality-affecting factors in laying hens: A review. *Czech J. Anim. Sci.* **2016**, *61*, 299–309. [CrossRef]
33. Tsai, W.; Yang, J.; Lai, C.; Cheng, Y.; Lin, C.; Yeh, C. Characterization and adsorption properties of eggshells and eggshell membrane. *Bioresour. Technol.* **2006**, *97*, 488–493. [CrossRef] [PubMed]
34. Walsh, P.P.; Banerjee, A.; Murphy, E. The UN 2030 Agenda for Sustainable Development. In *Partnerships and the Sustainable Development Goals*; Springer International Publishing: Cham, Switzerland, 2022; pp. 1–12.
35. Lin, T.-Y.; Chai, W.S.; Chen, S.-J.; Shih, J.-Y.; Koyande, A.K.; Liu, B.-L.; Chang, Y.-K. Removal of soluble microbial products and dyes using heavy metal wastes decorated on eggshell. *Chemosphere* **2021**, *270*, 128615. [CrossRef]
36. Liao, D.; Zheng, W.; Li, X.; Yang, Q.; Yue, X.; Guo, L.; Zeng, G. Removal of lead(II) from aqueous solutions using carbonate hydroxyapatite extracted from eggshell waste. *J. Hazard. Mater.* **2010**, *177*, 126–130. [CrossRef]
37. Liu, R.; Lian, B. Immobilisation of Cd(II) on biogenic and abiotic calcium carbonate. *J. Hazard. Mater.* **2019**, *378*, 120707. [CrossRef]
38. Wen, T.; Zhao, Y.; Zhang, T.; Xiong, B.; Hu, H.; Zhang, Q.; Song, S. Selective recovery of heavy metals from wastewater by mechanically activated calcium carbonate: Inspiration from nature. *Chemosphere* **2020**, *246*, 125842. [CrossRef]
39. Wang, G.; Liu, N.; Zhang, S.; Zhu, J.; Xiao, H.; Ding, C. Preparation and application of granular bentonite-eggshell composites for heavy metal removal. *J. Porous Mater.* **2022**, *29*, 817–826. [CrossRef]
40. Du, Y.; Lian, F.; Zhu, L. Biosorption of divalent Pb, Cd and Zn on aragonite and calcite mollusk shells. *Environ. Pollut.* **2011**, *159*, 1763–1768. [CrossRef]
41. Basaleh, A.A.; Al-Malack, M.H.; Saleh, T.A. Metal removal using chemically modified eggshells: Preparation, characterization, and statistical analysis. *Desalination Water Treat.* **2020**, *173*, 313–330. [CrossRef]
42. Ahmad, M.; Ahmad, M.; Usman, A.R.A.; Al-Faraj, A.S.; Abduljabbar, A.S.; Al-Wabel, M.I. Biochar composites with nano zerovalent iron and eggshell powder for nitrate removal from aqueous solution with coexisting chloride ions. *Environ. Sci. Pollut. Res.* **2018**, *25*, 25757–25771. [CrossRef] [PubMed]
43. Cao, H.; Wu, X.; Syed-Hassan, S.S.A.; Zhang, S.; Mood, S.H.; Milan, Y.J.; Garcia-Perez, M. Characteristics and mechanisms of phosphorous adsorption by rape straw-derived biochar functionalized with calcium from eggshell. *Bioresour. Technol.* **2020**, *318*, 124063. [CrossRef] [PubMed]
44. Guo, Z.; Li, J.; Guo, Z.; Guo, Q.; Zhu, B. Phosphorus removal from aqueous solution in parent and aluminum-modified eggshells: Thermodynamics and kinetics, adsorption mechanism, and diffusion process. *Environ. Sci. Pollut. Res.* **2017**, *24*, 14525–14536. [CrossRef] [PubMed]
45. Steiger, B.G.; Zhou, Z.; Anisimov, Y.A.; Evitts, R.W.; Wilson, L.D. Valorization of agro-waste biomass as composite adsorbents for sustainable wastewater treatment. *Ind. Crops Prod.* **2023**, *191*, 115913. [CrossRef]
46. Borhade, A.V.; Kale, A.S. Calcined eggshell as a cost effective material for removal of dyes from aqueous solution. *Appl. Water Sci.* **2017**, *7*, 4255–4268. [CrossRef]
47. Li, Z.L.; Wei, Y.D.; Wei, J.N.; Chen, K.Y.; He, Y.; Wang, M.M. Monodispersed $CaCO_3$@hydroxyapatite/magnetite microspheres for efficient and selective extraction of benzoylurea insecticides in tea beverages samples. *J. Hazard. Mater.* **2022**, *433*, 128754. [CrossRef]
48. Abdel-Khalek, M.; Rahman, M.A.; Francis, A. Exploring the adsorption behavior of cationic and anionic dyes on industrial waste shells of egg. *J. Environ. Chem. Eng.* **2017**, *5*, 319–327. [CrossRef]
49. Yusuff, A.S. Adsorption of cationic dye from aqueous solution using composite chicken eggshell—Anthill clay: Optimization of adsorbent preparation conditions. *Acta Polytech.* **2019**, *59*, 192–202. [CrossRef]
50. Ofudje, E.A.; Adeogun, I.A.; Idowu, M.A.; Kareem, S.O.; Ndukwe, N.A. Simultaneous removals of cadmium(II) ions and reactive yellow 4 dye from aqueous solution by bone meal-derived apatite: Kinetics, equilibrium and thermodynamic evaluations. *J. Anal. Sci. Technol.* **2020**, *11*, 7. [CrossRef]
51. Rajoriya, S.; Saharan, V.K.; Pundir, A.S.; Nigam, M.; Roy, K. Adsorption of methyl red dye from aqueous solution onto eggshell waste material: Kinetics, isotherms and thermodynamic studies. *Curr. Res. Green Sustain. Chem.* **2021**, *4*, 100180. [CrossRef]
52. Daraei, H.; Mittal, A.; Noorisepehr, M.; Daraei, F. Kinetic and equilibrium studies of adsorptive removal of phenol onto eggshell waste. *Environ. Sci. Pollut. Res.* **2013**, *20*, 4603–4611. [CrossRef] [PubMed]
53. Rápó, E.; Aradi, L.E.; Szabó, Á.; Posta, K.; Szép, R.; Tonk, S. Adsorption of Remazol Brilliant Violet-5R Textile Dye from Aqueous Solutions by Using Eggshell Waste Biosorbent. *Sci. Rep.* **2020**, *10*, 8385. [CrossRef] [PubMed]
54. Liu, X.; Shen, F.; Qi, X. Adsorption recovery of phosphate from aqueous solution by CaO-biochar composites prepared from eggshell and rice straw. *Sci. Total Environ.* **2019**, *666*, 694–702. [CrossRef] [PubMed]
55. Garduño-Pineda, L.; Linares-Hernández, I.; Solache-Ríos, M.J.; Teutli-Sequeira, A.; Martínez-Miranda, V. Removal of inorganic chemical species and organic matter from slaughterhouse wastewater via calcium acetate synthesized from eggshell. *J. Environ. Sci. Health Part A* **2019**, *54*, 295–305. [CrossRef]

56. Torit, J.; Phihusut, D. Phosphorus removal from wastewater using eggshell ash. *Environ. Sci. Pollut. Res.* **2019**, *26*, 34101–34109. [CrossRef]
57. Park, J.-H.; Choi, A.-Y.; Lee, S.-L.; Lee, J.-H.; Rho, J.-S.; Kim, S.-H.; Seo, D.-C. Removal of phosphates using eggshells and calcined eggshells in high phosphate solutions. *Appl. Biol. Chem.* **2022**, *65*, 75. [CrossRef]
58. Eletta, O.; Ajayi, O.; Ogunleye, O.; Akpan, I. Adsorption of cyanide from aqueous solution using calcinated eggshells: Equilibrium and optimisation studies. *J. Environ. Chem. Eng.* **2016**, *4*, 1367–1375. [CrossRef]
59. Sree, G.V.; Nagaraaj, P.; Kalanidhi, K.; Aswathy, C.; Rajasekaran, P. Calcium oxide a sustainable photocatalyst derived from eggshell for efficient photo-degradation of organic pollutants. *J. Clean. Prod.* **2020**, *270*, 122294. [CrossRef]
60. Lee, J.-I.; Hong, S.-H.; Lee, C.-G.; Park, S.-J. Fluoride removal by thermally treated egg shells with high adsorption capacity, low cost, and easy acquisition. *Environ. Sci. Pollut. Res.* **2021**, *28*, 35887–35901. [CrossRef]
61. Santos, A.F.; Arim, A.L.; Lopes, D.V.; Gando-Ferreira, L.M.; Quina, M.J. Recovery of phosphate from aqueous solutions using calcined eggshell as an eco-friendly adsorbent. *J. Environ. Manag.* **2019**, *238*, 451–459. [CrossRef]
62. Giraldo, L.; Moreno-Piraján, J.C. Study of adsorption of phenol on activated carbons obtained from eggshells. *J. Anal. Appl. Pyrolysis* **2014**, *106*, 41–47. [CrossRef]
63. Zafar, M.N.; Amjad, M.; Tabassum, M.; Ahmad, I.; Zubair, M. $SrFe_2O_4$ nanoferrites and $SrFe_2O_4$/ground eggshell nanocomposites: Fast and efficient adsorbents for dyes removal. *J. Clean. Prod.* **2018**, *199*, 983–994. [CrossRef]
64. El-Kemary, M.A.; El-Mehasseb, I.M.; Shoueir, K.R.; El-Shafey, S.E.; El-Shafey, O.I.; Aljohani, H.A.; Fouad, R.R. Sol-gel TiO_2 decorated on eggshell nanocrystal as engineered adsorbents for removal of acid dye. *J. Dispers. Sci. Technol.* **2018**, *39*, 911–921. [CrossRef]
65. Lin, P.-Y.; Wu, H.-M.; Hsieh, S.-L.; Li, J.-S.; Dong, C.; Chen, C.-W.; Hsieh, S. Preparation of vaterite calcium carbonate granules from discarded oyster shells as an adsorbent for heavy metal ions removal. *Chemosphere* **2020**, *254*, 126903. [CrossRef] [PubMed]
66. Choi, H.-J.; Lee, S.-M. Heavy metal removal from acid mine drainage by calcined eggshell and microalgae hybrid system. *Environ. Sci. Pollut. Res.* **2015**, *22*, 13404–13411. [CrossRef]
67. Sankaran, R.; Show, P.L.; Ooi, C.-W.; Ling, T.C.; Shu-Jen, C.; Chen, S.-Y.; Chang, Y.-K. Feasibility assessment of removal of heavy metals and soluble microbial products from aqueous solutions using eggshell wastes. *Clean Technol. Environ. Policy* **2020**, *22*, 773–786. [CrossRef]
68. Zhang, T.; Tu, Z.; Lu, G.; Duan, X.; Yi, X.; Guo, C.; Dang, Z. Removal of heavy metals from acid mine drainage using chicken eggshells in column mode. *J. Environ. Manag.* **2017**, *188*, 1–8. [CrossRef]
69. Liu, H.; Liu, Y.; Tang, L.; Wang, J.; Yu, J.; Zhang, H.; Yu, M.; Zou, J.; Xie, Q. Egg shell biochar-based green catalysts for the removal of organic pollutants by activating persulfate. *Sci. Total Environ.* **2020**, *745*, 141095. [CrossRef] [PubMed]
70. Hu, H.; Li, X.; Huang, P.; Zhang, Q.; Yuan, W. Efficient removal of copper from wastewater by using mechanically activated calcium carbonate. *J. Environ. Manag.* **2017**, *203*, 1–7. [CrossRef]
71. Seyahmazegi, E.N.; Mohammad-Rezaei, R.; Razmi, H. Multiwall carbon nanotubes decorated on calcined eggshell waste as a novel nano-sorbent: Application for anionic dye Congo red removal. *Chem. Eng. Res. Des.* **2016**, *109*, 824–834. [CrossRef]
72. Kanyal, M.; Bhatt, A.A. Removal of Heavy Metals from Water (Cu and Pb) Using Household Waste as an Adsorbent. *J. Bioremediat. Biodegrad.* **2015**, *6*, 1–6.
73. Wen, T.; Zhao, Y.; Zhang, T.; Xiong, B.; Hu, H.; Zhang, Q.; Song, S. Effect of anions species on copper removal from wastewater by using mechanically activated calcium carbonate. *Chemosphere* **2019**, *230*, 127–135. [CrossRef] [PubMed]
74. Waheed, M.; Yousaf, M.; Shehzad, A.; Inam-Ur-Raheem, M.; Khan, M.K.I.; Khan, M.R.; Ahmad, N.; Abdullah; Aadil, R.M. Channelling eggshell waste to valuable and utilizable products: A comprehensive review. *Trends Food Sci. Technol.* **2020**, *106*, 78–90. [CrossRef]
75. Majd, M.M.; Kordzadeh-Kermani, V.; Ghalandari, V.; Askari, A.; Sillanpää, M. Adsorption isotherm models: A comprehensive and systematic review (2010–2020). *Sci. Total Environ.* **2022**, *812*, 151334. [CrossRef]
76. Shukla, P.R.; Wang, S.; Ang, H.M.; Tadé, M.O. Synthesis, characterisation, and adsorption evaluation of carbon-natural-zeolite composites. *Adv. Powder Technol.* **2009**, *20*, 245–250. [CrossRef]
77. Barauskas, D.; Dzikaras, M.; Bieliauskas, D.; Pelenis, D.; Vanagas, G.; Viržonis, D. Selective ultrasonic gravimetric sensors based on capacitive micromachined ultrasound transducer structure—A review. *Sensors* **2020**, *20*, 3554. [CrossRef]
78. Subramanyam, B.; Das, A. Linearised and non-linearised isotherm models optimization analysis by error functions and statistical means. *J. Environ. Health Sci. Eng.* **2014**, *12*, 92. [CrossRef]
79. Parimal, S.; Prasad, M.; Bhaskar, U. Prediction of equillibrium sorption isotherm: Comparison of linear and nonlinear methods. *Ind. Eng. Chem. Res.* **2010**, *49*, 2882–2888. [CrossRef]
80. Osmari, T.A.; Gallon, R.; Schwaab, M.; Barbosa-Coutinho, E.; Severo, J.B., Jr.; Pinto, J.C. Statistical analysis of linear and non-linear regression for the estimation of adsorption isotherm parameters. *Adsorpt. Sci. Technol.* **2013**, *31*, 433–458. [CrossRef]
81. Kumar, K.V.; Porkodi, K.; Rocha, F. Isotherms and thermodynamics by linear and non-linear regression analysis for the sorption of methylene blue onto activated carbon: Comparison of various error functions. *J. Hazard. Mater.* **2008**, *151*, 794–804. [CrossRef]
82. Yan, F.; Chu, Y.; Zhang, K.; Zhang, F.; Bhandari, N.; Ruan, G.; Dai, Z.; Liu, Y.; Zhang, Z.; Kan, A.T.; et al. Determination of adsorption isotherm parameters with correlated errors by measurement error models. *Chem. Eng. J.* **2015**, *281*, 921–930. [CrossRef]
83. Al-Ghouti, M.A.; Da'Ana, D.A. Guidelines for the use and interpretation of adsorption isotherm models: A review. *J. Hazard. Mater.* **2020**, *393*, 122383. [CrossRef]

84. Cassol, G.O.; Gallon, R.; Schwaab, M.; Barbosa-Coutinho, E.; Júnior, J.B.S.; Pinto, J.C. Statistical evaluation of non-linear parameter estimation procedures for adsorption equilibrium models. *Adsorpt. Sci. Technol.* **2014**, *32*, 257–273. [CrossRef]
85. Langmuir, I. The adsorption of gases on plane surfaces of glass, mica and platinum. *J. Am. Chem. Soc.* **1918**, *40*, 1361–1403. [CrossRef]
86. Salam, O.E.A.; Reiad, N.A.; ElShafei, M.M. A study of the removal characteristics of heavy metals from wastewater by low-cost adsorbents. *J. Adv. Res.* **2011**, *2*, 297–303. [CrossRef]
87. Bessashia, W.; Berredjem, Y.; Hattab, Z.; Bououdina, M. Removal of Basic Fuchsin from water by using mussel powdered eggshell membrane as novel bioadsorbent: Equilibrium, kinetics, and thermodynamic studies. *Environ. Res.* **2020**, *186*, 109484. [CrossRef] [PubMed]
88. Adeogun, A.I.; Ofudje, E.A.; Idowu, M.A.; Kareem, S.O.; Vahidhabanu, S.; Babu, B.R. Biowaste-Derived Hydroxyapatite for Effective Removal of Reactive Yellow 4 Dye: Equilibrium, Kinetic, and Thermodynamic Studies. *ACS Omega* **2018**, *3*, 1991–2000. [CrossRef]
89. Chen, Y.; Zhu, Y.; Wang, Z.; Li, Y.; Wang, L.; Ding, L.; Gao, X.; Ma, Y.; Guo, Y. Application studies of activated carbon derived from rice husks produced by chemical-thermal process—A review. *Adv. Colloid Interface Sci.* **2011**, *163*, 39–52. [CrossRef]
90. Peterson, O.R.D.L. A useful adsorption isotherm. *J. Phys. Chem.* **1958**, *63*, 1024.
91. Sips, R. On the structure of a catalyst surface. *J. Chem. Phys.* **1948**, *16*, 490–495. [CrossRef]
92. Wang, J.; Guo, X. Adsorption kinetic models: Physical meanings, applications, and solving methods. *J. Hazard. Mater.* **2020**, *390*, 122156. [CrossRef] [PubMed]
93. Azizian, S.; Eris, S. Adsorption isotherms and kinetics. In *Interface Science and Technology*; Elsevier: Amsterdam, The Netherlands, 2021; pp. 445–509.
94. Tan, K.; Hameed, B. Insight into the adsorption kinetics models for the removal of contaminants from aqueous solutions. *J. Taiwan Inst. Chem. Eng.* **2017**, *74*, 25–48. [CrossRef]
95. Patel, H. Fixed-bed column adsorption study: A comprehensive review. *Appl. Water Sci.* **2019**, *9*, 45. [CrossRef]
96. Ho, Y.S.; McKay, G. Pseudo-second order model for sorption processes. *Process Biochem.* **1999**, *34*, 451–465. [CrossRef]
97. Oladoja, N.A.; Ahmad, A.L. Gastropod shell as a precursor for the synthesis of binary alkali-earth and transition metal oxide for Cr(VI) Abstraction from Aqua System. *Sep. Purif. Technol.* **2013**, *116*, 230–239. [CrossRef]
98. Kapoor, A.; Viraraghavan, T. Removal of heavy metals from aqueous solutions using immobilized fungal biomass in continuous mode. *Water Res.* **1998**, *32*, 1968–1977. [CrossRef]
99. Xu, Z.; Cai, J.-G.; Pan, B.-C. Mathematically modeling fixed-bed adsorption in aqueous systems. *J. Zhejiang Univ. Sci. A* **2013**, *14*, 155–176. [CrossRef]
100. Han, R.; Ding, D.; Xu, Y.; Zou, W.; Wang, Y.; Li, Y.; Zou, L. Use of rice husk for the adsorption of congo red from aqueous solution in column mode. *Bioresour. Technol.* **2008**, *99*, 2938–2946. [CrossRef]
101. Ko, D.C.K.; Porter, J.F.; Mckay, G. Optimised correlations for the fixed-bed adsorption of metal ions on bone char. *Chem. Eng. Sci.* **2000**, *55*, 5819–5829. [CrossRef]
102. Pincus, L.N.; Rudel, H.E.; Petrović, P.V.; Gupta, S.; Westerhoff, P.; Muhich, C.L.; Zimmerman, J.B. Exploring the Mechanisms of Selectivity for Environmentally Significant Oxo-Anion Removal during Water Treatment: A Review of Common Competing Oxo-Anions and Tools for Quantifying Selective Adsorption. *Environ. Sci. Technol.* **2020**, *54*, 9769–9790. [CrossRef]
103. Georgin, J.; Franco, D.S.; Martinello, K.d.B.; Lima, E.C.; Silva, L.F. A review of the toxicology presence and removal of ketoprofen through adsorption technology. *J. Environ. Chem. Eng.* **2022**, *10*, 107798. [CrossRef]
104. El Messaoudi, N.; Franco, D.S.P.; Gubernat, S.; Georgin, J.; Şenol, Z.M.; Ciğeroğlu, Z.; Allouss, D.; El Hajam, M. Advances and future perspectives of water defluoridation by adsorption technology: A review. *Environ. Res.* **2024**, *252*, 118857. [CrossRef] [PubMed]
105. Georgin, J.; Franco, D.S.P.; Ramos, C.G.; Piccilli, D.G.; Lima, E.C.; Sher, F. A review of the antibiotic ofloxacin: Current status of ecotoxicology and scientific advances in its removal from aqueous systems by adsorption technology. *Chem. Eng. Res. Des.* **2023**, *193*, 99–120. [CrossRef]
106. Pettinato, M.; Chakraborty, S.; Arafat, H.A.; Calabro', V. Eggshell: A green adsorbent for heavy metal removal in an MBR system. *Ecotoxicol. Environ. Saf.* **2015**, *121*, 57–62. [CrossRef]
107. Shaheen, S.M.; Eissa, F.I.; Ghanem, K.M.; El-Din, H.M.G.; Al Anany, F.S. Heavy metals removal from aqueous solutions and wastewaters by using various byproducts. *J. Environ. Manag.* **2013**, *128*, 514–521. [CrossRef]
108. Jaradat, A.Q.; Telfah, D.B.; Ismail, R. Heavy metals removal from landfill leachate by coagulation/flocculation process combined with continuous adsorption using eggshell waste materials. *Water Sci. Technol.* **2021**, *84*, 3817–3832. [CrossRef]
109. Hong, K.-S.; Lee, H.M.; Bae, J.S.; Ha, M.G.; Jin, J.S.; Hong, T.E.; Kim, J.P.; Jeong, E.D. Removal of Heavy Metal Ions by using Calcium Carbonate Extracted from Starfish Treated by Protease and Amylase. *J. Anal. Sci. Technol.* **2011**, *2*, 75–82. [CrossRef]
110. Makuchowska-Fryc, J. Use of The Eggshells in Removing Heavy Metals from Waste Water—The Process Kinetics and Efficiency. *Ecol. Chem. Eng. S* **2019**, *26*, 165–174. [CrossRef]
111. Zeng, C.; Hu, H.; Feng, X.; Wang, K.; Zhang, Q. Activating $CaCO_3$ to enhance lead removal from lead-zinc solution to serve as green technology for the purification of mine tailings. *Chemosphere* **2020**, *249*, 126227. [CrossRef]

112. Elabbas, S.; Mandi, L.; Berrekhis, F.; Pons, M.N.; Leclerc, J.P.; Ouazzani, N. Removal of Cr(III) from chrome tanning wastewater by adsorption using two natural carbonaceous materials: Eggshell and powdered marble. *J. Environ. Manag.* **2016**, *166*, 589–595. [CrossRef]
113. Hu, Q.; Chen, N.; Feng, C.; Hu, W. Nitrate adsorption from aqueous solution using granular chitosan-Fe^{3+} complex. *Appl. Surf. Sci.* **2015**, *347*, 1–9. [CrossRef]
114. Taghizadeh, M.; Asgharinezhad, A.A.; Samkhaniany, N.; Tadjarodi, A.; Abbaszadeh, A.; Pooladi, M. Solid phase extraction of heavy metal ions based on a novel functionalized magnetic multi-walled carbon nanotube composite with the aid of experimental design methodology. *Microchim. Acta* **2014**, *181*, 597–605. [CrossRef]
115. Islam, M.A.; Benhouria, A.; Asif, M.; Hameed, B. Methylene blue adsorption on factory-rejected tea activated carbon prepared by conjunction of hydrothermal carbonization and sodium hydroxide activation processes. *J. Taiwan Inst. Chem. Eng.* **2015**, *52*, 57–64. [CrossRef]
116. Islam, M.A.; Ahmed, M.J.; Khanday, W.A.; Asif, M.; Hameed, B.H. Mesoporous activated coconut shell-derived hydrochar prepared via hydrothermal carbonization-NaOH activation for methylene blue adsorption. *J. Environ. Manag.* **2017**, *203*, 237–244. [CrossRef]
117. Vijayaraghavan, K.; Won, S.W.; Yun, Y.-S. Treatment of complex Remazol dye effluent using sawdust- and coal-based activated carbons. *J. Hazard. Mater.* **2009**, *167*, 790–796. [CrossRef]
118. Bello, O.S.; Siang, T.T.; Ahmad, M.A. Adsorption of Remazol Brilliant Violet-5R reactive dye from aqueous solution by cocoa pod husk-based activated carbon: Kinetic, equilibrium and thermodynamic studies. *Asia-Pac. J. Chem. Eng.* **2012**, *7*, 378–388. [CrossRef]
119. Kaya, N. A comprehensive study on adsorption behavior of some azo dyes from aqueous solution onto different adsorbents. *Water Sci. Technol.* **2017**, *76*, 478–489. [CrossRef]
120. Rachna, K.; Agarwal, A.; Singh, N.B. Rice husk and Sodium hydroxide activated Rice husk for removal of Reactive yellow dye from water. *Mater. Today Proc.* **2019**, *12*, 573–580. [CrossRef]
121. Szlachta, M.; Wójtowicz, P. Adsorption of methylene blue and Congo red from aqueous solution by activated carbon and carbon nanotubes. *Water Sci. Technol.* **2013**, *68*, 2240–2248. [CrossRef]
122. Singh, P.; Raizada, P.; Pathania, D.; Sharma, G.; Sharma, P. Microwave induced KOH activation of guava peel carbon as an adsorbent for congo red dye removal from aqueous phase. *Indian J. Chem. Technol.* **2013**, *20*, 305–311.
123. Chavan, S.B.; Kumbhar, R.R.; Madhu, D.; Singh, B.; Sharma, Y.C. Synthesis of biodiesel from Jatropha curcas oil using waste eggshell and study of its fuel properties. *RSC Adv.* **2015**, *5*, 63596–63604. [CrossRef]
124. Pinto, L.F.; Montaño, A.M.; González, C.P.; Barón, G.C. Removal of rhodamine B in wastewater from the textile industry using geopolymeric material. *J. Phys. Conf. Ser.* **2019**, *1386*, 012040. [CrossRef]
125. Xiao, W.; Garba, Z.N.; Sun, S.; Lawan, I.; Wang, L.; Lin, M.; Yuan, Z. Preparation and evaluation of an effective activated carbon from white sugar for the adsorption of rhodamine B dye. *J. Clean. Prod.* **2020**, *253*, 119989. [CrossRef]
126. Ye, X.; Shang, S.; Zhao, Y.; Cui, S.; Zhong, Y.; Huang, L. Ultra-efficient adsorption of copper ions in chitosan–montmorillonite composite aerogel at wastewater treatment. *Cellulose* **2021**, *28*, 7201–7212. [CrossRef]
127. Ahmad, M.; Zhang, B.; Wang, J.; Xu, J.; Manzoor, K.; Ahmad, S.; Ikram, S. New method for hydrogel synthesis from diphenylcarbazide chitosan for selective copper removal. *Int. J. Biol. Macromol.* **2019**, *136*, 189–198. [CrossRef]
128. Salman, H.; Shaheen, H.; Abbas, G.; Khalouf, N. Use of Syrian natural zeolite for heavy metals removal from industrial waste water: Factors and mechanism. *J. Entomol. Zool. Stud.* **2017**, *5*, 452–461.
129. Wang, M.; Cai, H.; Zhang, J. Application research on the adsorption of cadmium ion in wastewater by zeolite molecular sieve. *Chem. Eng. Trans.* **2018**, *71*, 403–408.
130. El-Azim, H.A.; Mourad, F.A. Removal of Heavy Metals Cd (II), Fe (III) and Ni (II), from Aqueous Solutions by Natural (Clinoptilolite) Zeolites and Application to Industrial Wastewater. *Asian J. Environ. Ecol.* **2018**, *7*, 1–13. [CrossRef]
131. Moosa, A.A.; Ridha, A.M.; Hussien, N.A. Removal of Zinc Ions from Aqueous Solution by Bioadsorbents and CNTs. *Am. J. Mater. Sci.* **2016**, *6*, 105–114. [CrossRef]
132. Banu, H.A.T.; Karthikeyan, P.; Meenakshi, S. Removal of nitrate and phosphate ions from aqueous solution using zirconium encapsulated chitosan quaternized beads: Preparation, characterization and mechanistic performance. *Results Surf. Interfaces* **2021**, *3*, 100010. [CrossRef]
133. Jung, K.-W.; Hwang, M.-J.; Ahn, K.-H.; Ok, Y.-S. Kinetic study on phosphate removal from aqueous solution by biochar derived from peanut shell as renewable adsorptive media. *Int. J. Environ. Sci. Technol.* **2015**, *12*, 3363–3372. [CrossRef]
134. Wang, Z.; Shi, M.; Li, J.; Zheng, Z. Influence of moderate pre-oxidation treatment on the physical, chemical and phosphate adsorption properties of iron-containing activated carbon. *J. Environ. Sci.* **2014**, *26*, 519–528. [CrossRef] [PubMed]
135. Park, J.-H.; Wang, J.J.; Xiao, R.; Zhou, B.; Delaune, R.D.; Seo, D.-C. Effect of pyrolysis temperature on phosphate adsorption characteristics and mechanisms of crawfish char. *J. Colloid Interface Sci.* **2018**, *525*, 143–151. [CrossRef] [PubMed]
136. Solgi, M.; Mohamed, M.H.; Udoetok, I.A.; Steiger, B.G.; Wilson, L.D. Evaluation of a granular Cu-modified chitosan biocomposite for sustainable sulfate removal from aqueous media: A batch and fixed-bed column study. *Int. J. Biol. Macromol.* **2024**, *260*, 129275. [CrossRef]
137. Steiger, B.G.K.; Bui, N.T.; Babalola, B.M.; Wilson, L.D. Sustainable agro-waste pellets as granular slow-release fertilizer carrier systems for ammonium sulfate. *RSC Sustain.* **2024**, *2*, 2979–2988. [CrossRef]

138. Alimohammadi, V.; Sedighi, M.; Jabbari, E. Optimization of sulfate removal from wastewater using magnetic multi-walled carbon nanotubes by response surface methodology. *Water Sci. Technol.* **2017**, *76*, 2593–2602. [CrossRef]
139. Runtti, H.; Tynjälä, P.; Tuomikoski, S.; Kangas, T.; Hu, T.; Rämö, J.; Lassi, U. Utilisation of barium-modified analcime in sulphate removal: Isotherms, kinetics and thermodynamics studies. *J. Water Process. Eng.* **2017**, *16*, 319–328. [CrossRef]
140. Camacho, L.M.; Torres, A.; Saha, D.; Deng, S. Adsorption equilibrium and kinetics of fluoride on sol–gel-derived activated alumina adsorbents. *J. Colloid Interface Sci.* **2010**, *349*, 307–313. [CrossRef]
141. Choong, C.E.; Wong, K.T.; Jang, S.B.; Nah, I.W.; Choi, J.; Ibrahim, S.; Yoon, Y.; Jang, M. Fluoride removal by palm shell waste based powdered activated carbon vs. functionalized carbon with magnesium silicate: Implications for their application in water treatment. *Chemosphere* **2020**, *239*, 124765. [CrossRef]
142. Yang, W.; Li, C.; Tian, S.; Liu, L.; Liao, Q. Influence of synthesis variables of a sol-gel process on the properties of mesoporous alumina and their fluoride adsorption. *Mater. Chem. Phys.* **2020**, *242*, 122499. [CrossRef]
143. Demiral, H.; Gündüzoğlu, G. Removal of nitrate from aqueous solutions by activated carbon prepared from sugar beet bagasse. *Bioresour. Technol.* **2010**, *101*, 1675–1680. [CrossRef] [PubMed]
144. Kamarehie, B.; Aghaali, E.; Musavic, S.A.; Hashemi, S.Y.; Jafari, A. Nitrate removal from aqueous solutions using granular activated carbon modified with iron nanoparticles. *Int. J. Eng.* **2018**, *31*, 554–563. [CrossRef]
145. Zhu, D.; Zuo, J.; Jiang, Y.; Zhang, J.; Zhang, J.; Wei, C. Carbon-silica mesoporous composite in situ prepared from coal gasification fine slag by acid leaching method and its application in nitrate removing. *Sci. Total. Environ.* **2020**, *707*, 136102. [CrossRef] [PubMed]
146. Kausar, A.; Zohra, S.T.; Ijaz, S.; Iqbal, M.; Iqbal, J.; Bibi, I.; Nouren, S.; El Messaoudi, N.; Nazir, A. Cellulose-based materials and their adsorptive removal efficiency for dyes: A review. *Int. J. Biol. Macromol.* **2023**, *224*, 1337–1355. [CrossRef]
147. Namasivayam, C.; Sureshkumar, M.V. Removal of chromium(VI) from water and wastewater using surfactant modified coconut coir pith as a biosorbent. *Bioresour. Technol.* **2008**, *99*, 2218–2225. [CrossRef]
148. Zheng, B.; Qian, L.; Yuan, H.; Xiao, D.; Yang, X.; Paau, M.C.; Choi, M.M. Preparation of gold nanoparticles on eggshell membrane and their biosensing application. *Talanta* **2010**, *82*, 177–183. [CrossRef]
149. Dong, Q.; Su, H.; Cao, W.; Zhang, D.; Guo, Q.; Lai, Y. Synthesis and characterizations of hierarchical biomorphic titania oxide by a bio-inspired bottom-up assembly solution technique. *J. Solid State Chem.* **2007**, *180*, 949–955. [CrossRef]
150. Mallakpour, S.; Tabesh, F.; Hussain, C.M. Water decontamination using $CaCO_3$ nanostructure and its nanocomposites: Current advances. *Polym. Bull.* **2023**, *80*, 7201–7219. [CrossRef]
151. Yang, D.; Qi, L.; Ma, J. Eggshell membrane templating of hierarchically ordered macroporous networks composed of TiO_2 tubes. *Adv. Mater.* **2002**, *14*, 1543–1546. [CrossRef]
152. Intharapat, P.; Kongnoo, A.; Kateungngan, K. The Potential of Chicken Eggshell Waste as a Bio-filler Filled Epoxidized Natural Rubber (ENR) Composite and its Properties. *J. Polym. Environ.* **2013**, *21*, 245–258. [CrossRef]
153. Moonlek, B.; Saenboonruang, K. Mechanical and electrical properties of radiation-vulcanized natural rubber latex with waste eggshell powder as bio-fillers. *Radiat. Eff. Defects Solids* **2019**, *174*, 452–466. [CrossRef]
154. Niju, S.; Meera, K.; Begum, S.; Anantharaman, N. Modification of egg shell and its application in biodiesel production. *J. Saudi Chem. Soc.* **2014**, *18*, 702–706. [CrossRef]
155. Wijaya, V.T. Evaluation of Eggshell as Organic Fertilizer on Sweet Basil. *Int. J. Sustain. Agric. Res.* **2019**, *6*, 79–86.
156. Lee, Y.; Kim, A.Y.; Min, S.; Kwak, H. Characteristics of milk tablets supplemented with nanopowdered eggshell or oyster shell. *Int. J. Dairy Technol.* **2016**, *69*, 337–345. [CrossRef]
157. Than, M.M.; Lawanprasert, P.; Jateleela, S. Utilization of eggshell powder as excipient in fast and sustained release acetaminophen tablets. *Mahidol. Univ. J. Pharm. Sci.* **2012**, *39*, 32–38.
158. Asma, T.; Bakar, A.; Rosly, M.F.; Ain, S.; Jafar, M. Eggshell coated grey cast iron for corrosion applications. *J. Teknol.* **2017**, *79*, 1–6. [CrossRef]
159. Yuan, X.; Wu, L.; He, X.; Zeinu, K.; Huang, L.; Zhu, X.; Hou, H.; Liu, B.; Hu, J.; Yang, J. Separator modified with N,S co-doped mesoporous carbon using egg shell as template for high performance lithium-sulfur batteries. *Chem. Eng. J.* **2017**, *320*, 178–188. [CrossRef]
160. Fina, B.L.; Brun, L.R.; Rigalli, A. Increase of calcium and reduction of lactose concentration in milk by treatment with kefir grains and eggshell. *Int. J. Food Sci. Nutr.* **2016**, *67*, 133–140. [CrossRef]
161. Choi, H.-J. Efficiency of methyl-esterified eggshell membrane biomaterials for intensified microalgae harvesting. *Environ. Eng. Res.* **2017**, *22*, 356–362. [CrossRef]
162. Kismiati, S.; Yuwanta, T.; Zuprizal, Z.; Supadmo, S. THE performance of laying hens fed different calcium source. *J. Indones. Trop. Anim. Agric.* **2012**, *37*, 263–270. [CrossRef]
163. King'ori, A. A Review of the Uses of Poultry Eggshells and Shell Membranes. *Int. J. Poult. Sci.* **2011**, *10*, 908–912. [CrossRef]
164. Sunardi, S.; Ariawan, D.; Surojo, E.; Prabowo, A.R.; Akbar, H.I.; Cao, B.; Carvalho, H. Assessment of eggshell-based material as a green-composite filler: Project milestones and future potential as an engineering material. *J. Mech. Behav. Mater.* **2023**, *32*, 20220269. [CrossRef]
165. Mallakpour, S.; Khadem, E. Chitosan/$CaCO_3$-silane nanocomposites: Synthesis, characterization, in vitro bioactivity and Cu(II) adsorption properties. *Int. J. Biol. Macromol.* **2018**, *114*, 149–160. [CrossRef] [PubMed]

166. Li, H.; Sun, J.; Jiang, Q.; Xia, H.; Cheng, S.; Zhou, Z.; Nie, X.; Zhao, C. Facile, time-saving cigarette butt-assisted combustion synthesis of modified CaO-based sorbents for high-temperature CO_2 capture. *Fuel* **2023**, *337*, 126868. [CrossRef]
167. Chen, G.; Shan, R.; Shi, J.; Yan, B. Ultrasonic-assisted production of biodiesel from transesterification of palm oil over ostrich eggshell-derived CaO catalysts. *Bioresour. Technol.* **2014**, *171*, 428–432. [CrossRef]
168. Vall, M.; Hultberg, J.; Strømme, M.; Cheung, O. Inorganic carbonate composites as potential high temperature CO_2 sorbents with enhanced cycle stability. *RSC Adv.* **2019**, *9*, 20273–20280. [CrossRef]
169. Knowles, G.P.; Chaffee, A.L. Shaped Silica-polyethyleneimine Composite Sorbents for CO_2 Capture via Adsorption. *Energy Procedia* **2017**, *114*, 2219–2227. [CrossRef]
170. Rattanakunsong, N.; Jullakan, S.; Płotka-Wasylka, J.; Bunkoed, O. A hierarchical porous composite magnetic sorbent of reduced graphene oxide embedded in polyvinyl alcohol cryogel for solvent-assisted-solid phase extraction of polycyclic aromatic hydrocarbons. *J. Sep. Sci.* **2022**, *45*, 1774–1783. [CrossRef]
171. Shapkin, N.P.; Surkov, M.V.; Tutov, M.V.; Khalchenko, I.G.; Fedorets, A.N.; Sharshina, E.A.; Razov, V.I.; Tokar, E.A.; Papynov, E.K. Organo-Inorganic Composites Based on Phosphorus Vermiculite and Resorcinol–Formaldehyde Polymer and Their Use for Sorption of Nonradioactive Strontium from Solutions. *Russ. J. Inorg. Chem.* **2022**, *67*, 221–230. [CrossRef]
172. Zaharia, M.-M.; Vasiliu, A.-L.; Trofin, M.-A.; Pamfil, D.; Bucatariu, F.; Racovita, S.; Mihai, M. Design of multifunctional composite materials based on acrylic ion exchangers and CaCO3 as sorbents for small organic molecules. *React. Funct. Polym.* **2021**, *166*, 104997. [CrossRef]
173. Choi, D.; Shin, J.; Park, Y. Effects of $CaCl_2$ on cyclic carbonation-calcination kinetics of CaO-based composite for potential application to solar thermochemical energy storage. *Chem. Eng. Sci.* **2021**, *230*, 116207. [CrossRef]
174. Chabane, L.; Bouras, O. Experimental design approach in optimizing the sorption properties of a new generation of reinforced porous hybrid beads. *Arab. J. Chem.* **2020**, *13*, 6461–6471. [CrossRef]
175. Bunia, I.; Socoliuc, V.; Vekas, L.; Doroftei, F.; Varganici, C.; Coroaba, A.; Simionescu, B.C.; Mihai, M. Superparamagnetic Composites Based on Ionic Resin Beads/$CaCO_3$/Magnetite. *Chem.—Eur. J.* **2016**, *22*, 18036–18044. [CrossRef]
176. Bhaskar, T.; Uddin, A.; Kaneko, J.; Kusaba, T.; Matsui, T.; Muto, A.; Sakata, Y.; Murata, K. Liquefaction of mixed plastics containing PVC and dechlorination by calcium-based sorbent. *Energy Fuels* **2002**, *17*, 75–80. [CrossRef]
177. Bhaskar, T.; Matsui, T.; Nitta, K.; Uddin, A.; Muto, A.; Sakata, Y. Laboratory evaluation of calcium-, iron-, and potassium-based carbon composite sorbents for capture of hydrogen chloride gas. *Energy Fuels* **2002**, *16*, 1533–1539. [CrossRef]
178. Mostafa, M.M.; El Saied, M.; Morshedy, A.S. Novel Calcium Carbonate-titania nanocomposites for enhanced sun light photo catalytic desulfurization process. *J. Environ. Manag.* **2019**, *250*, 109462. [CrossRef] [PubMed]
179. Toro, P.; Quijada, R.; Yazdani-Pedram, M.; Arias, J.L. Eggshell, a new bio-filler for polypropylene composites. *Mater. Lett.* **2007**, *61*, 4347–4350. [CrossRef]
180. Xu, Y.; Hanna, M. Effect of eggshell powder as nucleating agent on the structure, morphology and functional properties of normal corn starch fooms. *Packag. Technol. Sci.* **2007**, *20*, 165–172. [CrossRef]
181. Ji, G.; Zhu, H.; Qi, C.; Zeng, M. Mechanism of interactions of eggshell microparticles with epoxy resins. *Polym. Eng. Sci.* **2009**, *49*, 1383–1388. [CrossRef]
182. Kang, D.J.; Pal, K.; Park, S.J.; Bang, D.S.; Kim, J.K. Effect of eggshell and silk fibroin on styrene–ethylene/butylene–styrene as bio-filler. *Mater. Des.* **2010**, *31*, 2216–2219. [CrossRef]
183. Tangboriboon, N.; Pannangpetch, W.; Aranyik, K.; Petcharoen, K.; Sirivat, A. Embedded Eggshells as a Bio-Filler in Natural Rubber for Thermal Insulation Composite Foams. *Prog. Rubber Plast. Recycl. Technol.* **2015**, *31*, 189–205. [CrossRef]
184. Di Serio, M.; Tesser, R.; Pengmei, L.; Santacesaria, E. Heterogeneous catalysts for biodiesel production. *Energy Fuels* **2008**, *22*, 207–217. [CrossRef]
185. Huber, G.W.; Iborra, S.; Corma, A. Synthesis of transportation fuels from biomass: Chemistry, catalysts, and engineering. *Chem. Rev.* **2006**, *106*, 4044–4098. [CrossRef] [PubMed]
186. Ma, F.; Hanna, M.A. Biodiesel production: A review. *Bioresour. Technol.* **1999**, *70*, 1–15. [CrossRef]
187. Balázsi, C.; Wéber, F.; Kövér, Z.; Horváth, E.; Németh, C. Preparation of calcium–phosphate bioceramics from natural resources. *J. Eur. Ceram. Soc.* **2007**, *27*, 1601–1606. [CrossRef]
188. Sharma, Y.C.; Singh, B.; Korstad, J. Application of an efficient nonconventional heterogeneous catalyst for biodiesel synthesis from pongamia pinnata oil. *Energy Fuels* **2010**, *24*, 3223–3231. [CrossRef]
189. Cho, Y.B.; Seo, G. High activity of acid-treated quail eggshell catalysts in the transesterification of palm oil with methanol. *Bioresour. Technol.* **2010**, *101*, 8515–8519. [CrossRef]
190. Navajas, A.; Issariyakul, T.; Arzamendi, G.; Gandía, L.; Dalai, A. Development of eggshell derived catalyst for transesterification of used cooking oil for biodiesel production. *Asia-Pac. J. Chem. Eng.* **2013**, *8*, 742–748. [CrossRef]
191. Mostafavi, E.; Mahinpey, N.; Rahman, M.; Sedghkerdar, M.H.; Gupta, R. High-purity hydrogen production from ash-free coal by catalytic steam gasification integrated with dry-sorption CO_2 capture. *Fuel* **2016**, *178*, 272–282. [CrossRef]
192. Taufiq-Yap, Y.H.; Wong, P.; Marliza, T.S.; Suziana, N.M.N.; Tang, L.H.; Sivasangar, S. Hydrogen production from wood gasification promoted by waste eggshell catalyst. *Int. J. Energy Res.* **2013**, *37*, 1866–1871. [CrossRef]
193. Mosaddegh, E. Ultrasonic-assisted preparation of nano eggshell powder: A novel catalyst in green and high efficient synthesis of 2-aminochromenes. *Ultrason. Sonochem.* **2013**, *20*, 1436–1441. [CrossRef] [PubMed]

194. Mosaddegh, E.; Hassankhani, A. Preparation and characterization of nano-CaO based on eggshell waste: Novel and green catalytic approach to highly efficient synthesis of pyrano [4,3-b]pyrans. *Cuihua Xuebao/Chin. J. Catal.* **2014**, *35*, 351–356. [CrossRef]
195. Dayanidhi, K.; Sheik Eusuff, N. Fabrication, Characterization, and Evaluation of Eggshells as a Carrier for Sustainable Slow-Release Multi-Nutrient Fertilizers. *ACS Appl. Bio Mater.* **2021**, *4*, 8215–8224. [CrossRef] [PubMed]
196. Borges, R.; Giroto, A.S.; Klaic, R.; Wypych, F.; Ribeiro, C. Mechanochemical synthesis of eco-friendly fertilizer from eggshell (calcite) and KH_2PO_4. *Adv. Powder Technol.* **2021**, *32*, 4070–4077. [CrossRef]
197. Dayanidhi, K.; Vadivel, P.; Jothi, S.; Eusuff, N.S. White Eggshells: A Potential Biowaste Material for Synergetic Adsorption and Naked-Eye Colorimetric Detection of Heavy Metal Ions from Aqueous Solution. *ACS Appl. Mater. Interfaces* **2020**, *12*, 1746–1756. [CrossRef] [PubMed]